ISSN 2096-7071
CN 10-1629/R1

CHINA CDC WEEKLY

Vol. 4 No. 26 Jul. 1, 2022

中国疾病预防控制中心周报

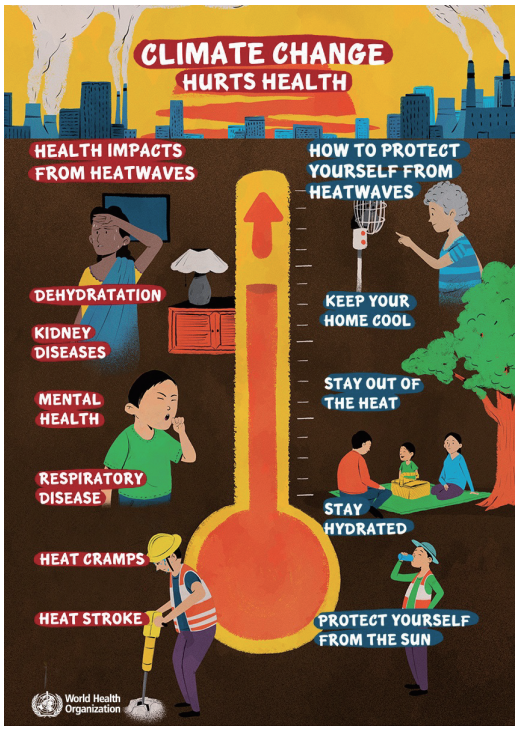

ENVIRONMENTAL HEALTH ISSUE

Preplanned Studies

Vital Surveillances

Review

ISSN 2096-7071
9 772096 707224 26>

Preplanned Studies

Long-Term Temperature Variability and Risk of Dyslipidemia Among Middle-Aged and Elderly Adults: A Prospective Cohort Study — China, 2011–2018

Jianbo Jin[1]; Yuxin Wang[1]; Zhihu Xu[1]; Ru Cao[1]; Hanbin Zhang[3]; Qiang Zeng[2]; Xiaochuan Pan[1]; Jing Huang[1,4,#]; Guoxing Li[1,3,#]

Summary

What is already known about this topic?

Long-term temperature variability (TV) has been examined to be associated with cardiovascular disease (CVD). TV-related dyslipidemia helps us understand the mechanism of how climate change affects CVD.

What is added by this report?

Based on the China Health and Retirement Longitudinal Study (CHARLS) from 2011 to 2018, this study estimated the long-term effect of TV on dyslipidemia in middle-aged and elderly adults.

What are the implications for public health practice?

This study suggested that long-term TV may increase the risk of dyslipidemia. With the threat of climate change, these findings have great significance for making policies and adaptive strategies to reduce relevant risk of CVD.

Dyslipidemia is a vital risk factor for cardiovascular disease (CVD) and has increased considerably in recent years. Temperature was convinced to be a major climate factor that affected plasma lipid levels (*1*). In 2021, Kang et al. suggested long-term temperature variability (TV), an indicator of extreme temperatures, increased the risk of CVD; furthermore, dyslipidemia can modify the long-term TV-related risk of CVD (*2*). Lao et al. also found that the variation of dyslipidemia prevalence showed seasonal features in China (*3*). However, as an indicator of climate change, TV was rarely included in exploring its impacts on dyslipidemia. Therefore, we evaluated the long-term effect of TV on dyslipidemia in middle-aged and older adults based on the China Health and Retirement Longitudinal Study (CHARLS) from 2011 to 2018.

The study data were collected from 17,596 individual participants in 150 county-level units sampled from 450 communities in 125 cities among 28 provincial-level administrative divisions (PLADs) of China selecting by the multi-stage probability sampling method. We excluded 1,615 participants with dyslipidemia, 5,753 participants without dyslipidemia reports, and 609 participants for the lack of key covariate information. The final analysis sample included 9,619 individuals without dyslipidemia at baseline with key variables in 2011–2018 (Supplementary Figure S1, available in http://weekly.chinacdc.cn/). In CHARLS, all participants provided written informed consent.

This study defined the dependent variable as being diagnosed with dyslipidemia or not at baseline. Diagnosed dyslipidemia was defined as participants' self-reports of ever having been diagnosed with dyslipidemia by doctors. The daily meteorological information of all selected cities in the same period (2011–2018) was obtained from the China Meteorological Science Data Sharing Service Network. Nearest-neighbour interpolation was applied to estimate the daily data across the mainland of China at a spatial resolution of a regular grid of 10 km × 10 km (ten-fold cross validation: R^2=0.95; root mean square error=2.34 ℃). We calculated the annual standard deviation (SD) of the daily average temperature as the TV index, and TV of the year before each survey was considered as the long-term TV exposure. TV data were assigned to each participant by their residential cities and survey year. Annual average concentrations of fine particles with a diameter ≤2.5 μm ($PM_{2.5}$) from 2011 to 2018 were calculated from a combination of satellite observations, chemical transport modeling, and ground-based monitoring (R^2=0.81; slope=0.90) (*4*). We assigned the annual average city-level $PM_{2.5}$ concentration of the year before each survey to each participant.

Recorded demographic characteristics (age, sex) in CHARLS were included in covariates. We also collated three lifestyle covariates (smoking, alcohol drinking, social interactions) and three socioeconomic status

covariates (education attainment, residence, and household income per capita). Household income status was divided into binaries by average. Educational attainment was divided by whether junior school education was attained. Gross domestic product (GDP) at the city level was also collected from the National Bureau of Statistics and China's National Knowledge Infrastructure. By the Kunlun-Qinling-Huaihe line, the cities were divided into southern cities and northern cities. Environmental variables and dependent variables were time-varying for each survey, and other covariables were the values at baseline.

We assessed the association between long-term TV and the incidence of dyslipidemia using time-varying Cox proportional hazards model on a year-based time scale. We first evaluated the effects of TV on a continuous scale and reported the association with per 1 ℃ increase in TV. According to a previous study about long-term TV (*2*), TV was also divided into three categories (low<8.03 ℃, medium=8.03–10.23 ℃, high>10.23 ℃), with the low TV as the reference group. We tested the statistical significance of the linear trend between each category of TV and dyslipidemia.

We fitted three models with different categories of covariates, and TV was included as a continuous variable or categorical variable in the models. Punitive spline regression (df=3) was used to analyse the exposure-response curve of TV and dyslipidemia. Furthermore, we evaluated the modification in the association between long-term TV and dyslipidemia, stratifying by age, sex, residency, household income status, education attainment, and geographical location.

Data arrangement, cleaning, and all statistical analyses were conducted using R (version 4.0.2, R Foundation for Statistical Computing, Vienna, Austria) with packages dplyr, survival, smoothHR, and coxme. Statistical significance was defined as P<0.05, two sides. We included 9,619 participants without dyslipidemia and found 1,848 of them with dyslipidemia during the follow-up period. The median follow-up time was 4 years [interquartile range (IQR): 2–7 years]. In cities of CHARLS, the average annual TV between 2011 and 2018 ranged from 4.18 ℃ to 17.75 ℃. Participants living with high TV were more likely to have higher education attainment, live in urban areas, smoke more, drink less, and have higher $PM_{2.5}$ exposure and higher incidence of dyslipidemia (Supplementary Table S1, available in http://weekly.chinacdc.cn/).

We observed a positive association between dyslipidemia and long-term exposure to TV in three models (details about the models can be found in Table 1). In model 3, we observed 8.3% [95% confidence interval (CI): 4.2%–12.6%] increase in dyslipidemia for each 1 ℃ increase in TV (Table 1). Compared with low TV levels, the increase in medium and high TV levels was associated with 34.0% (95% CI: 15.6%–55.3%) and 57.9% (95% CI: 30.3%–91.3%) higher risks of dyslipidemia in a significant positive trend (Table 1). We also did a sensitivity analysis using the interval years of TV between surveys as long-term exposure and found that hazard ratio (HR) was 1.079 (95% CI: 1.036–1.123) (Table 1). Punitive spline regression with 3 degrees of freedom showed that exposure-response curve of long-term TV exposure and dyslipidemia was almost linear (Figure 1).

Marginal significant difference was found in the long-term TV-related risk between participants with low education attainment (HR: 1.093; 95% CI: 1.011–1.181) and high education attainment (HR: 1.084; 95% CI: 1.036–1.134) (Interaction P value=0.053) (Supplementary Table S2, available in http://weekly.chinacdc.cn/). No significant difference

TABLE 1. Cox regression models of TV and dyslipidemia among middle-aged and elderly adults, 2011–2018.

Models	TV per 1 ℃ increment [Hazard ratio (95%CI)]	TV levels [Hazard ratio (95%CI)]			*P*
		Low	Medium	High	
Model 1*	1.089 (1.071–1.107)	1.00 (Ref)	1.346 (1.167–1.553)	1.566 (1.301–1.885)	<0.001
Model 2†	1.093 (1.052–1.136)	1.00 (Ref)	1.340 (1.156–1.553)	1.579 (1.303–1.913)	<0.001
Model 3§	1.083 (1.042–1.126)	1.00 (Ref)	1.338 (1.153–1.553)	1.583 (1.303–1.924)	<0.001
Model 4¶	1.079 (1.036–1.123)	1.00 (Ref)	1.279 (1.106–1.478)	1.389 (1.148–1.681)	<0.001

Abbreviations: CI=confidence interval; $PM_{2.5}$=particulate matter of diameter ≤2.5 μm; TV=temperature variability.

* Crude model.

† Adjusted for model 1 criteria and age, sex, whether having lifestyle of smoking, drinking, annual average temperature, $PM_{2.5}$, GDP.

§ Adjusted for model 2 criteria and residency, household income per capita, educational attainment.

¶ Adjusted for model 3 criteria, using the interval years of TV between surveys as long-term exposure.

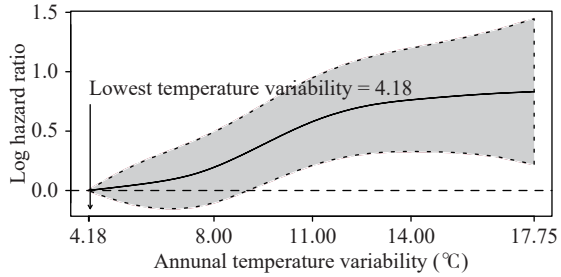

FIGURE 1. The exposure-response curve of long-term TV and dyslipidemia among middle-aged and elderly adults — China, 2011–2018.
Notes: Age, sex, marriage status, having disability, smoking, drinking, having accident injury, and having social interactions were adjusted. The solid line represents log hazard ratio, and the gray zone indicates 95% confidence interval.
Abbreviation: TV=temperature variability.

was found in the long-term TV effects in age, sex, residence, household income status, and living in different geographical regions.

DISCUSSION

In this study, we found a positive near-linear association between TV and risk the of dyslipidemia in middle-aged and elderly people. TV might affect the incidence of dyslipidemia, the risk factor of CVD.

Previous studies focused more on TV-related mortality or the incidence of CVD. A study analysed the effects of short-term TV among 31 cities in China, and observed a 1 ℃ rise of TV would increase 0.98 of CVD mortality (*5*). Shi et al. study in the USA found that for each 1 ℃ increase in TV, mortality in summer and winter increased by 0.80 and 0.41, respectively (*6*). A study in China with 35,000 participants over 35 years found that per 1 ℃ increase of long-term TV was associated with 6 increased incidence of CVD, and dyslipidemia was possibly a modifying factor (*2*). In this current study, we observed that higher TV would increase the incidence of dyslipidemia, which helps to understand the effects of long-term TV on CVD, especially among middle-aged and elderly populations. However, further studies were needed to examine the cause-and-effect relationship among long-term TV, dyslipidemia, and CVD.

Limited researches had been carried out to explore the underlying mechanism. Several studies suggested that extreme ambient temperature might affect the levels of high-density lipoprotein (HDL) and low-density lipoprotein (LDL), possibly by disturbing the absorbing of lipid (*7–8*). Some mechanistic studies showed that the unstable temperature would affect other blood biomarkers, such as blood cholesterol levels and plasma fibrinogen concentrations (*5*). The fluctuation in ambient temperature due to climate change would result in an imbalance between energy intake and energy expenditure, which contributes to the prevalence of metabolic syndrome (*9–10*). The mechanism of how TV affects plasma lipid levels needs further investigation.

The study was subject to some limitations. First, because of the limitation of geographical information, exposure of TV was assessed at the city level, which might have induced exposure misclassification. Second, since the research object was the middle-aged and elderly people over 45 years old, the results could not represent the impact of long-term TV on dyslipidemia in younger people. Third, the long-term exposure could be affected by other potential unknown confounding factors, such as indoor air-conditioner use, which might have led to inaccurate estimation.

In conclusion, we observed that long-term exposure to TV may increase the risk of dyslipidemia. Under the challenges of climate change and aging of population, these findings provided implications for making policies and adaptive strategies, such as providing extreme temperature warnings and plans to protect people working outdoors. Further studies are needed to investigate the underlying mechanisms for the reported association.

Conflicts of interest: No conflicts of interest.

Acknowledgements: China Center for Economic Research, National School of Development, Peking University, Beijing, China.

Funding: Supported by from National Natural Science Foundation Project of China (81872590 and 41761144056).

doi: 10.46234/ccdcw2022.122

[#] Corresponding authors: Jing Huang, jing_huang@bjmu.edu.cn; Guoxing Li, liguoxing@bjmu.edu.cn.

[1] Department of Occupational and Environmental Health Sciences, Peking University School of Public Health, Beijing, China; [2] Department of Occupational Disease Control and Prevention, Tianjin Centers for Disease Control and Prevention, Tianjin, China; [3] Environmental Research Group, MRC Centre for Environment and Health, Imperial College London, London, the United Kingdom; [4] Deep Medicine, Nuffield Department of Women's and Reproductive Health, University of Oxford, Oxford OX1 2BQ, the United Kingdom.

Submitted: December 17, 2021; Accepted: June 15, 2022

REFERENCES

1. Zhou XM, Lin HY, Zhang SG, Ren JW, Wang Z, Zhang Y, et al.

Effects of climatic factors on plasma lipid levels: a 5-year longitudinal study in a large Chinese population. J Clin Lipidol 2016;10(5):1119 – 28. http://dx.doi.org/10.1016/j.jacl.2016.06.009.
2. Kang YT, Tang HS, Zhang LF, Wang S, Wang X, Chen Z, et al. Long-term temperature variability and the incidence of cardiovascular diseases: a large, representative cohort study in China. Environ Pollut 2021;278:116831. http://dx.doi.org/10.1016/j.envpol.2021.116831.
3. Lao JH, Liu YF, Yang Y, Peng P, Ma FF, Ji S, et al. Time series decomposition into dyslipidemia prevalence among urban Chinese population: secular and seasonal trends. Lipids Health Dis 2021;20(1):114. http://dx.doi.org/10.1186/s12944-021-01541-6.
4. Hammer MS, Van Donkelaar A, Li C, Lyapustin A, Sayer AM, Hsu NC, et al. Global estimates and long-term trends of fine particulate matter concentrations (1998-2018). Environ Sci Technol 2020;54(13):7879 – 90. http://dx.doi.org/10.1021/acs.est.0c01764.
5. Yang J, Zhou MG, Li MM, Liu XB, Yin P, Sun QH, et al. Vulnerability to the impact of temperature variability on mortality in 31 major Chinese cities. Environ Pollut 2018;239:631 – 7. http://dx.doi.org/10.1016/j.envpol.2018.04.090.
6. Shi LH, Liu PF, Wang Y, Zanobetti A, Kosheleva A, Koutrakis P, et al. Chronic effects of temperature on mortality in the Southeastern USA using satellite-based exposure metrics. Sci Rep 2016;6(1):30161. http://dx.doi.org/10.1038/srep30161.
7. Halonen JI, Zanobetti A, Sparrow D, Vokonas PS, Schwartz J. Outdoor temperature is associated with serum HDL and LDL. Environ Res 2011;111(2):281 – 7. http://dx.doi.org/10.1016/j.envres.2010.12.001.
8. Mathew AV, Yu J, Guo YH, Byun J, Chen YE, Wang L, et al. Effect of ambient fine particulate matter air pollution and colder outdoor temperatures on high-density lipoprotein function. Am J Cardiol 2018;122(4):565 – 70. http://dx.doi.org/10.1016/j.amjcard.2018.04.061.
9. Turner JB, Kumar A, Koch CA. The effects of indoor and outdoor temperature on metabolic rate and adipose tissue – the Mississippi perspective on the obesity epidemic. Rev Endocr Metab Disord 2016;17(1):61 – 71. http://dx.doi.org/10.1007/s11154-016-9358-z.
10. Wang TY, Zhou H, Sun QH. Fluctuation in ambient temperature: interplay between brown adipose tissue, metabolic health, and cardiovascular diseases. Environ Dis 2016;1(1):3 – 13. http://dx.doi.org/10.4103/2468-5690.180334.

SUPPLEMENTARY MATERIAL

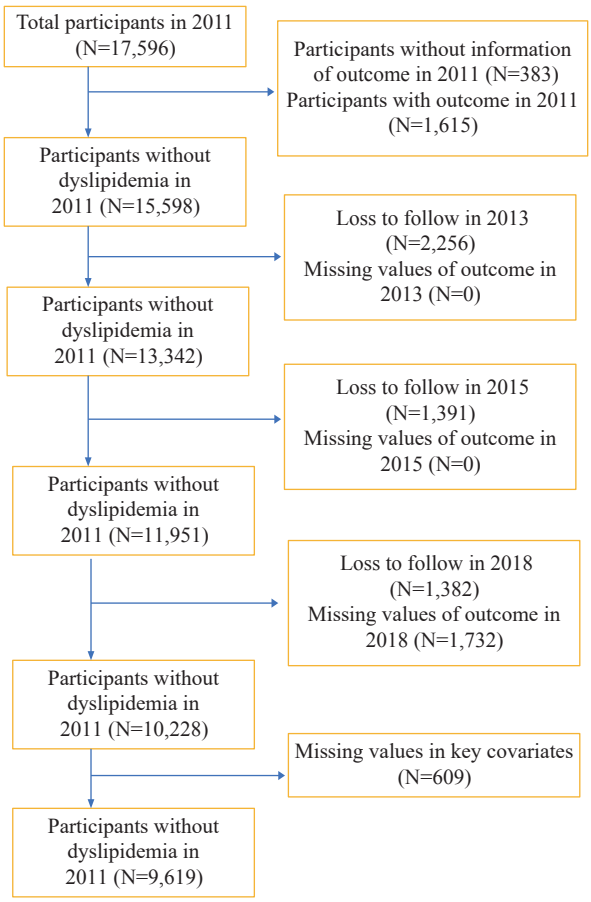

SUPPLEMENTARY FIGURE S1. Flowchart of the study samples.

SUPPLEMENTARY TABLE S1. Comparison of the characteristics between included and excluded individuals among middle-aged and elderly adults — China, 2011–2018.

Characteristic	Excluded individuals (N=7,977)		Included individuals (N=9,619)		*P*
	No.	Percentage (%)	No.	Percentage (%)	
Age ≥65 (years)	2,440	30.59	2,315	24.07	<0.001
Male	3,959	49.63	4,470	46.47	<0.001
Smoking					<0.001
Current smoker	2,438	30.56	2,903	30.18	–
Former smoker	616	7.72	556	5.78	–
Never smoker	4,886	61.25	6,160	64.04	–
Drinking					0.330
Never drinker	4,668	58.52	5,675	59.00	–
Rare drinker	835	10.47	949	9.87	–
Regular drinker	2,431	30.48	2,995	31.14	–
Having social interactions					<0.001
Daily interactions	1,820	22.82	2,173	22.59	–
Weekly interactions	754	9.45	1,093	11.36	–
Occasional interactions	781	9.79	1,380	14.35	–
No interactions	3,124	39.16	4,973	51.70	–
Primary school and below	5,045	63.24	6,667	69.31	<0.001
Urban residency	3,864	48.44	3,233	33.61	<0.001
High household income	2,816	35.30	2,529	26.29	<0.001
Living in the south	4,134	51.82	5,259	54.67	<0.001
$PM_{2.5}$ (μg/m^3), Mean±SD	49.94±23.08		51.29±23.31		<0.001
Air temperature (℃), Mean±SD	14.07±5.54		14.53±5.15		<0.001
Long-term TV (℃), Mean±SD	9.88±2.57		9.60±2.39		<0.001

Note: "–" means not applicable.
Abbreviations: $PM_{2.5}$=particulate matter of diameter ≤2.5 μm; SD=standard deviation; TV=temperature variability.

SUPPLEMENTARY TABLE S2. The association between long-term TV and dyslipidemia in stratified analyses — China, 2011−2018.

Characteristics	Subgroup	Hazard ratio (95% CI)	*P* value
Sex	Male	1.094 (1.030, 1.162)	Ref.
	Female	1.073 (1.019, 1.129)	0.453
Age	<65 years	1.079 (1.033, 1.127)	Ref.
	≥65 years	1.095 (1.004, 1.195)	0.978
Residency	Rural	1.092 (1.042, 1.145)	Ref.
	Urban	1.094 (1.017, 1.176)	0.324
Household income	Below average	1.086 (1.040, 1.134)	Ref.
	Above average	1.080 (0.984, 1.185)	0.579
Education attainment	Primary school and below	1.093 (1.011, 1.181)	Ref.
	Junior school and above	1.084 (1.036, 1.134)	0.053
Region	Living in northern cities	1.078 (1.016, 1.145)	Ref.
	Living in southern cities	1.087 (1.017, 1.163)	0.312

Notes: Model 3 adjustment (as illustrated in the Table 1 footnote) was used for the stratified analyses.
Abbreviations: TV=temperature variability; CI=confidence interval; Ref.=reference.

Preplanned Studies

Independent and Interactive Effects of Environmental Conditions on Aerosolized Surrogate SARS-CoV-2 — Beijing, China, June to September 2020

Yixin Mao[1,&]; Yueyun Luo[2,&]; Wenda Zhang[3,&]; Pei Ding[1]; Xia Li[1]; Fuchang Deng[1]; Kaiqiang Xu[1]; Min Hou[1]; Cheng Ding[1]; Youbin Wang[1]; Zhaomin Dong[4,5]; Raina MacIntyre[6]; Xiaoyuan Yao[1]; Song Tang[7,#]; Dongqun Xu[1,#]

Summary

What is already known about this topic?

Environmental factors such as temperature and humidity play important roles in the transmission of severe acute respiratory syndrome coronavirus 2 (SARS-CoV-2) via droplets/aerosols.

What is added by this report?

Higher relative humidity (61%–80%), longer spreading time (120 min), and greater dispersal distance (1 m) significantly reduced SARS-CoV-2 pseudovirus loads. There was an interaction effect between relative humidity and spreading time.

What are the implications for public health practice?

The findings contribute to our understanding of the impact of environmental factors on the transmission of SARS-CoV-2 via airborne droplets/aerosols.

Coronavirus disease 2019 (COVID-19) has led to a global pandemic and has highlighted the role of environmental factors in the transmission of severe acute respiratory syndrome coronavirus 2 (SARS-CoV-2) via droplets/aerosols. By altering the size distribution and evaporation rate of aerosols, temperature and relative humidity (RH) affect the shape and length of airborne trajectories (*1*). However, few studies have considered the interactions between multiple environmental factors and their combined impact on virus-laden droplets and aerosols.

Between June and September 2020, an orthogonal design was used to conduct suspension experiments in a 1.5 m × 1.0 m × 1.2 m laboratory exposure chamber. Independent and interactive impacts of temperature, RH, and distance on suspension time of droplets/aerosols with varying diameters and rates of size reduction of virus-laden droplets/aerosols size were explored. The numbers of droplets/aerosols with different diameters and reductions in viral load were measured in suspension and residual assays. We varied exposure chamber temperature from 16 ℃–28 ℃, RH from 30%–80%, and spreading distances of 0.5 m and 1 m to obtain data during 120 min after spreading sneeze-generated droplets/aerosols containing SARS-CoV-2 pseudovirus.

Droplets/aerosols settlement velocities increased over time under each temperature, RH, and distance range (Figure 1). With increasing time, larger aerosol particles (>1 μm) settled faster than smaller particles (<0.5 μm). After 120 min, approximately 50% of small particles (<0.5 μm) remained in suspension. Aerosol particles with diameters of >3 μm settled faster at lower RH (30%–45%), and there was a stepwise effect on aerosol particles with diameters of <0.5 μm with higher RH values (Figure 1). Aerosols remained in suspension in air currents longer than larger particles, but the numbers of suspended smaller particles decreased fastest at the highest RH range of 61%–80%.

Despite many studies on RH, few have investigated the relationship between temperature and stability of SARS-CoV-2 in aerosols. We found little difference between settling velocities of aerosols <0.5 μm in diameter under different temperature conditions compared with differences under varying RH values (Figure 1). However, particles >1 μm settled faster at higher temperatures (24 ℃–28 ℃) than at lower temperatures. Unlike variation in settling velocity from RH and temperature differences, settling velocities varied little by distances of 0.5 m and 1 m — a finding that might have been due to the relatively short (1 m) maximal dispersal distance we studied.

At the temperatures and distances studied, the lowest residual viral loads in droplets and aerosols at high RHs (61%–80%) were observed after 120 min (Table 1), suggesting that the highest RH range reduced viral loads (Figure 2A). Based on multiple

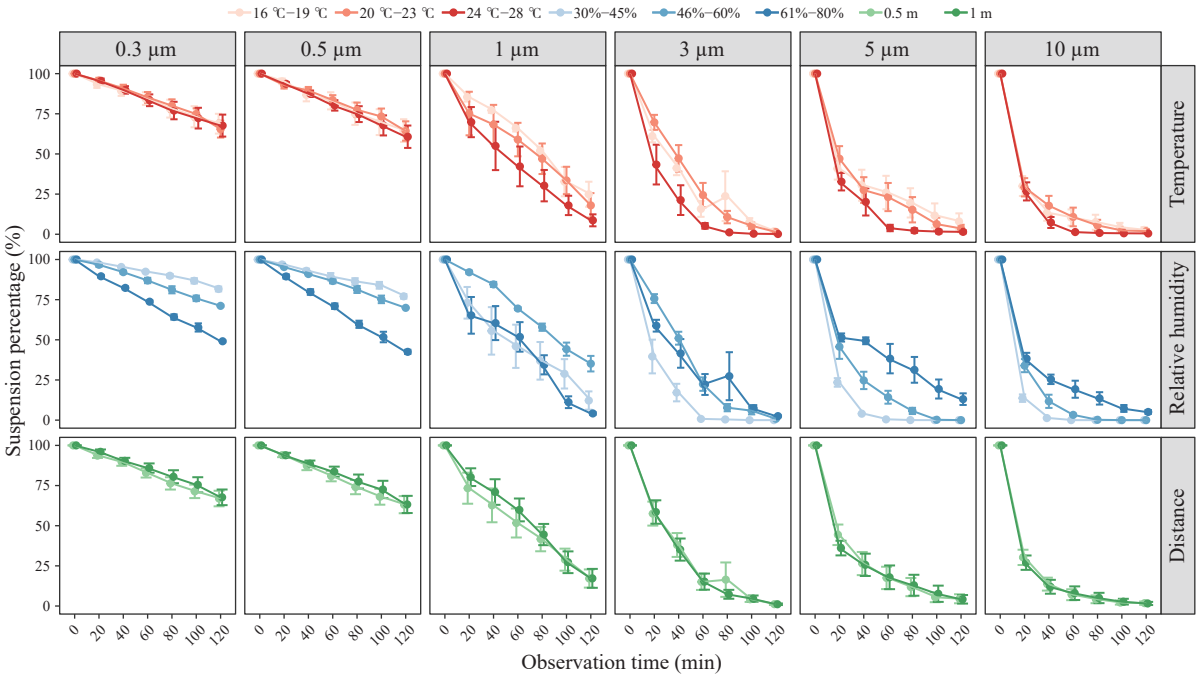

FIGURE 1. Suspension percentages of virus-laden droplet and aerosol particles with different diameters (0.3 μm, 0.5 μm, 1 μm, 3 μm, 5 μm, and 10 μm) under different conditions as a function of observation time.
Note: Environmental conditions include temperatures of 16 ℃–19 ℃, 20 ℃–23 ℃, and 24 ℃–48 ℃; relative humidity ranges of 30%–45%, 46%–60%, and 61%–80%; and spreading distances of 0.5 m and 1 m. Means and standard errors (mean±SE) are shown for three experimental replicates.

TABLE 1. Percentage of residual viral load in virus-laden droplets/aerosols under different environmental conditions at different observation time.

Experiment	T (℃)	RH (%)	Viral load (Log_{10} copies)				Percentage of residual viral load after 120 min (%)	
			0.5 m		1 m		0.5 m	1 m
			0 min	120 min	0 min	120 min	120 min *vs.* 0 min	120 min *vs.* 0 min
1	16–19	30–45	6.83	4.80	6.46	4.45	70.28	68.89
2	16–19	46–60	6.75	4.74	5.86	4.68	66.22	79.86
3	16–19	61–80	6.86	3.91	5.97	3.56	60.00	59.63
4	20–23	30–45	6.57	4.57	6.81	4.61	69.96	67.69
5	20–23	46–60	6.73	4.70	6.80	4.70	69.84	68.93
6	20–23	61–80	6.88	4.13	6.80	4.04	60.03	59.41
7	24–28	30–45	6.78	4.57	6.46	4.72	67.40	73.07
8	24–28	46–60	6.71	4.56	6.37	4.53	67.96	70.64
9	24–28	61–80	6.81	4.46	6.54	3.91	65.49	59.79

Notes: Environmental conditions include temperatures of 16 ℃–19 ℃, 20 ℃–23 ℃, and 24 ℃–48 ℃; RH ranges of 30%–45%, 46%–60%, and 61%–80%; and spreading distances of 0.5 m and 1 m.
Abbreviations: T=temperature, RH=relative humidity.

linear regression analysis, a time of 120 min and a spreading distance of 1 m significantly reduced droplet/aerosol viral loads (Figure 2A), with the most significant reduction factor being time. Mean viral loads after 120 min at distances of 0.5 m and 1 m were 66.33% and 67.81% of the mean viral loads at 0 min (Table 1).

We observed a significant interaction effect of time (120 min) and RH (61%–80%) on viral load (Figure 2C). There were no other statistically significant two-way or three-way interactions (Figure 2B, 2D, and 2E). According to modeling results, residual viral load decreased at high RH (61%–80%), while an increase in time (120 min)

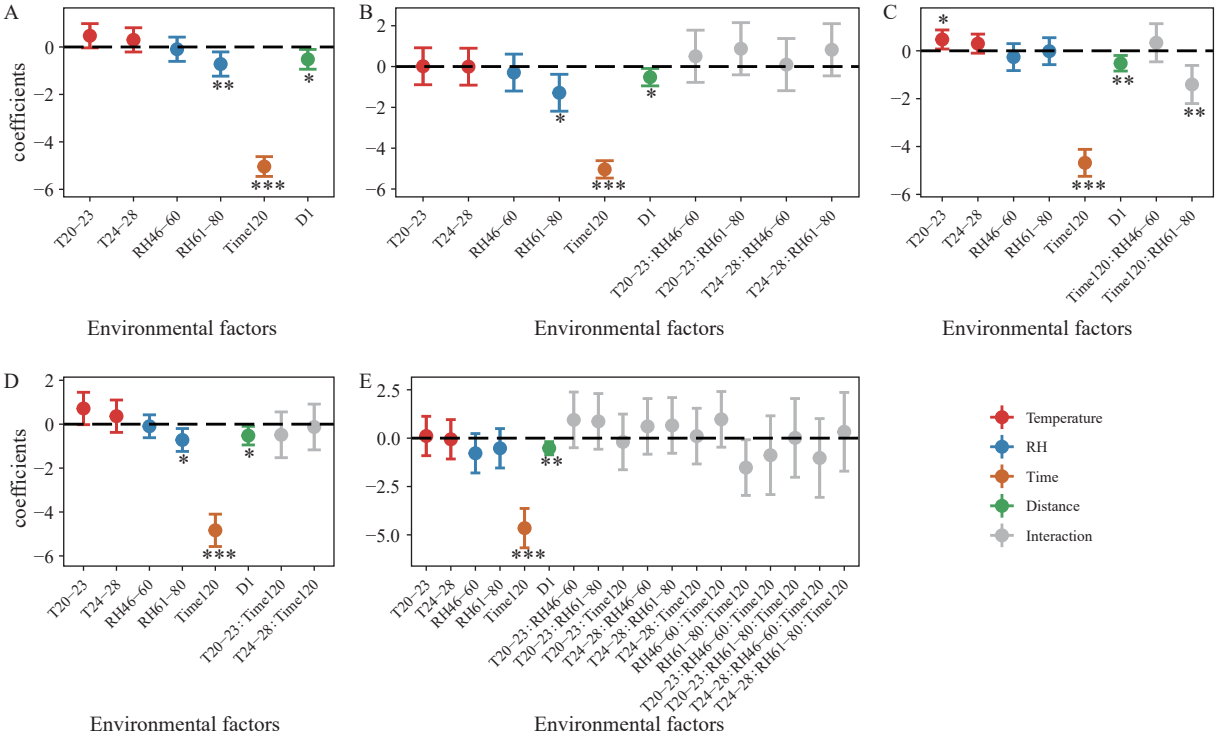

FIGURE 2. Modeled viral loads of virus-laden droplets/aerosols based on multiple interaction combinations of different environmental factors. (A) Multiple linear regression for independent factors; (B) two-way interaction between temperature and RH; (C) two-way interaction between time and RH; (D) two-way interaction between temperature and time; (E) three-way interaction among time, temperature, and RH.
Notes: Correlation refers to correlation coefficients and has no unit; T20–23 indicates the temperature was 20 ℃–23 ℃, and T24–28 indicates the temperature was 24 ℃–28 ℃; RH46–60 indicates relative humidity was 46%–60%, and RH61–80 indicates relative humidity was 61%–80%; Time120 indicates the interaction time was 120 min; and D1 indicates the spreading distance was 1 m.
Abbreviations: T=temperature, RH=relative humidity.
*: significance levels of $P<0.05$;
**: significance levels of $P<0.01$;
***: significance levels of $P<0.001$.

significantly affected the impact of RH on the viral load. Our results also showed that viral load was also significantly correlated with large particle size (≥3 μm) (Supplementary Figure S1, available in https://weekly.chinacdc.cn/), indicating that SARS-CoV-2 was mostly suspended within particles of this size class during sneezing.

DISCUSSION

The results showed that larger aerosol particles settled faster than smaller particles. The amount of small particles dicreased faster with higher relative hmidity. At high RHs, small droplets can uptake water vapor (*2*) and/or cohere to each other to form larger droplets, thus increasing their weight and size (*3*) and, therefore, increasing their settling rate. In contrast, aerosol particles with greater diameters (>3 μm) settled out faster at lower RHs (30%–45%). Higher RHs (61%–80%) significantly increased the settling velocity of aerosols with smaller diameters (<0.5 μm) and simultaneously reduced the viral load at any temperature or distance, implying that RH plays a significant role in the spread of SARS-CoV-2. The risk of transmitting SARS-CoV-2 via aerosols is higher in dry indoor environments. Therefore, this risk might be reduced by regulating the RH of indoor environments.

We also found that particles larger than 1 μm settled more rapidly at higher temperatures (24 ℃–28 ℃). High temperatures increased the evaporation of water and the conversion of respiratory droplets into aerosols. Hence, relatively high temperatures may affect large particles in a similar way that low RH values do. In addition, the mean viral loads after 120 min at different distances (0.5 m or 1 m) remained high. Time had a significant effect on viral loads, so this

finding may indicate a long suspension time and potentially long-range infection through the air (*4*). But the distances we studied (0.5 m or 1 m) had little effect on aerosol particle settlement. Thus, further studies involving larger distances are required to clarify the importance of distance on aerosol transmission.

Our findings are consistent with conclusions from other studies. Larger aerosol particles (>1 μm) settled faster, consistent with a study by Lindsley and colleagues (*5*). Approximately half of the small particles (<0.5 μm) remained suspended after 120 min. Respirable viral aerosols can linger and remain viable in air for relatively long periods (<16 h) owing to their smaller size (*6*). The number of smaller particles decreased fastest at the highest RHs. Similarly, a study of influenza virus found that exhaled respiratory droplets contributed to the propagation of influenza virus at a high RH (80%) (*7*). However, our maximum observation distance was small, and the difference in viral loads at different distances was not apparent. A previous study in hospital wards in Wuhan found that SARS-CoV-2-laden aerosols could spread over a distance of up to 4 m (*8*). A modeling simulation study reported that the maximum spreading distance of droplets could reach 6 m in an extremely cold and humid environment (*1*).

The study was subject to some limitations. First, due to bio-safety concerns, the study used a SARS-CoV-2 pseudovirus instead of SARS-CoV-2 to generate droplets and aerosols. Therefore, infectivity of the virus under different environmental conditions could not be determined. Second, the experiments were performed in a laboratory exposure chamber within a quiescent indoor environment, which was not necessarily representative of real exposure scenarios. Third, high viral loads were reported for the Delta and Omicron variants of SARS-CoV-2 (*9*), and these variants of concern (VOCs) were prone to spreading quickly in enclosed spaces (*10*). However, we did not consider the potential differences in the stabilities and transmission of these VOCs and/or variants of interest under different environmental conditions.

This study found that temperature, RH, spreading time, and dispersal distance, as well as the interaction between RH and spreading time, significantly affect the transmission of SARS-CoV-2 pseudovirus via droplets/aerosols. These findings highlighted the independent and interactive effects of environmental factors on virus-laden droplets and aerosols. By elucidating the effects of different environmental conditions on the trajectory of airborne viral transmission, adaptive public health strategies for preventing and controlling COVID-19 could incorporate seasonal weather variations and local environments. In order to reduce viral load and duration in the air, the following targeted preventive control measures might be adopted: 1) appropriately increase air humidity in residential and confined public places (e.g., using humidifiers); 2) appropriately increase ambient temperature; 3) increase the frequency of air disinfection; and 4) expand the scope of disinfection. Our study provided useful information for policymakers and guidance for the general public in the global combat against COVID-19.

Conflicts of Interest: No conflict of interest.

Acknowledgments: Special thanks to Dr. X. Shi from NIEH, China CDC for his tremendous support and guidance of this study, and Dr. S. Yang from University of South Carolina and T. Liu from South China Institute of Environmental Science for supporting on statistical analyses.

Funding: Supported by the Key Program of National Natural Science Foundation of China (No. 92043201) and the National Natural Science Foundation of China (No. 52091544), the Capital's Funds for Health Improvement and Research (No. 2021-1G-2172), the Young Scholar Scientific Research Foundation of National Institute of Environmental Health (NIEH), Chinese Center for Disease Control and Prevention (China CDC, No. 2020YSRF-03), and the COVID-19 Emergency Funding from NIEH, China CDC (No. GWTX05) and Bureau of Disease Prevention and Control, National Health Commission of China (No. WJW2102-01).

doi: 10.46234/ccdcw2022.123

[#] Corresponding authors: Song Tang, tangsong.2003@163.com; Dongqun Xu, xudq@chinacdc.cn.

[1] China CDC Key Laboratory of Environment and Population Health, National Institute of Environmental Health, Chinese Center for Disease Control and Prevention, Beijing, China; [2] Chinese Center for Disease Control and Prevention, Beijing, China; [3] University of South Carolina, Columbia, SC, USA; [4] School of Space and Environment, Beihang University, Beijing, China; [5] Beijing Advanced Innovation Center for Big Data-Based Precision Medicine, Beihang University, Beijing, China; [6] The Kirby Institute, Faculty of Medicine, The University of New South Wales, Sydney, NSW, Australia; [7] Center for Global Health, School of Public Health, Nanjing Medical University, Nanjing, Jiangsu Province, China.
[&] Joint first authors.

Submitted: May 06, 2022; Accepted: June 16, 2022

REFERENCES

1. Zhao L, Qi YH, Luzzatto-Fegiz P, Cui Y, Zhu YY. COVID-19: effects

of environmental conditions on the propagation of respiratory droplets. Nano Lett 2020;20(10):7744 – 50. http://dx.doi.org/10.1021/acs.nanolett.0c03331.
2. Hamed A, Korhonen H, Sihto SL, Joutsensaari J, Järvinen H, Petäjä T, et al. The role of relative humidity in continental new particle formation. J Geophys Res Atmos 2011;116(D3):D03202. http://dx.doi.org/10.1029/2010JD014186.
3. Shadloo-Jahromi A, Bavi O, Hossein Heydari M, Kharati-Koopaee M, Avazzadeh Z. Dynamics of respiratory droplets carrying SARS-CoV-2 virus in closed atmosphere. Results Phys 2020;19:103482. http://dx.doi.org/10.1016/j.rinp.2020.103482.
4. Alsved M, Bourouiba L, Duchaine C, Löndahl J, Marr LC, Parker ST, et al. Natural sources and experimental generation of bioaerosols: challenges and perspectives. Aerosol Sci Technol 2020;54(5):547 – 71. http://dx.doi.org/10.1080/02786826.2019.1682509.
5. Lindsley WG, Blachere FM, Thewlis RE, Vishnu A, Davis KA, Cao G, et al. Measurements of airborne influenza virus in aerosol particles from human coughs. PLoS One 2010;5(11):e15100. http://dx.doi.org/10.1371/journal.pone.0015100.
6. Fears AC, Klimstra WB, Duprex P, Hartman A, Weaver SC, Plante KS, et al. Persistence of severe acute respiratory syndrome coronavirus 2 in aerosol suspensions. Emerg Infect Dis 2020;26(9):2168 – 71. http://dx.doi.org/10.3201/eid2609.201806.
7. Lowen AC, Mubareka S, Steel J, Palese P. Influenza virus transmission is dependent on relative humidity and temperature. PLoS Pathog 2007;3(10):e151. http://dx.doi.org/10.1371/journal.ppat.0030151.
8. Guo ZD, Wang ZY, Zhang SF, Li X, Li L, Li C, et al. Aerosol and surface distribution of severe acute respiratory syndrome coronavirus 2 in hospital wards, Wuhan, China, 2020. Emerg Infect Dis 2020;26(7):1583 – 91. http://dx.doi.org/10.3201/eid2607.200885.
9. Lee BU. Why does the SARS-CoV-2 Delta VOC spread so rapidly? Universal conditions for the rapid spread of respiratory viruses, minimum viral loads for viral aerosol generation, effects of vaccination on viral aerosol generation, and viral aerosol clouds. Int J Environ Res Public Health 2021;18(18):9804. http://dx.doi.org/10.3390/ijerph18189804.
10. Riediker M, Briceno-Ayala L, Ichihara G, Albani D, Poffet D, Tsai DH, et al. Higher viral load and infectivity increase risk of aerosol transmission for Delta and Omicron variants of SARS-CoV-2. Swiss Med Wkly 2022;152:w30133. http://dx.doi.org/10.4414/smw.2022.w30133.

SUPPLEMENTARY MATERIAL

Materials and Methods

Study design: The orthogonal experiment was designed with two main aims. First, a suspension assay was used to investigate the impacts of environmental conditions on the suspension rates of pseudovirus-laden droplets and aerosols with different diameters. Second, a residual assay was used to determine the independent and interactive effects of environmental conditions on the viral loads of droplets/aerosols. The experimental conditions included temperature ranges of 16 ℃–19 ℃, 20 ℃–23 ℃, and 24 ℃–28 ℃; RH ranges of 30%–45%, 46%–60%, and 61%–80%; and spreading distances of 0.5 m and 1 m from the outlet of a sneezing simulation device. For the particle suspension assay, the observation times (i.e., durations after aerosolization) were 0 min, 20 min, 40 min, 60 min, 80 min, 100 min, and 120 min; 0 min and 120 min were selected for the residual assay. A SARS-CoV-2 spike pseudovirus (Sino Biological Inc., Beijing, China) without autonomous replication ability was used as a proxy for SARS-CoV-2 to determine the impact of each environmental factor on the viral loads of droplets/aerosols. According to a previous study (*1*), all experiments began with a similar viral concentration in artificial saliva suspensions and a similar number of sneeze-produced aerosol particles.

Experimental setup: Experiments were carried out in a laboratory exposure chamber (1.5 m × 1.0 m × 1.2 m) equipped with a high-efficiency filter to ensure the cleanliness of initial air under a quiescent environment (*2–3*). A temperature regulator (Jingchuang, RCW-360WIFI, China) and a humidity regulator (Soleusair, AHU-300N1, USA) were used to adjust the temperature and RH conditions, respectively, before each experiment according to the orthogonal experimental design. Dark conditions were maintained in the chamber throughout the experiments to avoid the potential influence of natural ultraviolet rays. We constructed a sneeze aerosol simulator comprising a compressor, an automated (on/off) electrical modulating valve, a manual electrical modulating valve, and a spray gun (*2–3*). The automated electrical modulating valve controlled the sneezing duration to 1 s. The manual electrical modulating valve adjusted the sneezing flow rate to 11±2 m/s, the total number of droplets/aerosols (diameters of 0.1 μm–100 μm) to 10^6, and the total aerosol volume to 70 μL/sneeze. To avoid cross-contamination, the chamber was ventilated with clean air [high-efficiency particulate air (HEPA)] during each test. After each test, the internal part of the chamber was wiped with 75% ethanol and then left to dry under clean air conditions.

Particle suspension assay: The poly-disperse SARS-CoV-2 pseudovirus solution was ejected 5 times (simulating 5 sneezes) from artificial saliva (10^8 copies/mL). The real-time particle number concentration (PNC) was measured with diameters ranging from 0.3 μm to >10 μm during each simulated sneeze. Particle measurement devices were set up at two different distances (0.5 m and 1 m away from the sneeze outlet). The sampling inlets of all devices were positioned along the centerline facing the sneeze outlet. At each sampling location, a Y09-301 Laser Particle Counter (AC-DC, Jiangsu Sujing Group Co., Ltd., China) was used to monitor the PNC. The data logging interval were set to 1s for all experiments. The testing times were 0 min, 20 min, 40 min, 60 min, 80 min, 100 min, and 120 min after each simulated sneeze. To determine potential variations, tests were repeated three times (n=3).

Residual assay of the viral load: Virus-laden droplets and aerosols were collected using bio-aerosol samplers (BIOSAMPLER, SKC, California, USA; sampling flow of 12.5 L/min and sampling frequency of 10 min) at 0 min and 120 min to detect the viral load. The obtained SARS-CoV-2 pseudovirus on the filter membranes was eluted with 1 mL of viral preservation medium (Dakewe Biological Engineering Co. Ltd, Shenzhen, China). Viral ribonucleic acid (RNA) was extracted using a QIAamp Viral RNA Mini Kit (QIAGEN Inc., Hilden, Germany) following the relevant protocol. The copy number of viral RNA was measured using a QX200 droplet digital polymerase chain reaction (ddPCR) system (Bio-Rad, California, USA) targeting the *WPRE* gene. Detailed information on the viral RNA extraction process, primer and probe sequences, reaction mix, droplet digital ddPCR amplification parameters, and quality assurance and quality control (QA/QC) can be found elsewhere (*2–3*).

Statistical analyses: Multiple linear regression analysis was performed using R (version 3.6.2, R core team 2021. A language and environment for statistical computing. R Foundation for Statistical Computing, Vienna, Austria. URL https://www.R-project.org/) to determine the relationship between each environmental factor and the viral load. First, we examined the effects of different temperature ranges (16 ℃–19 ℃, 20 ℃–23 ℃, and 24 ℃–28 ℃), RHs (30%–45%, 46%–60%, and 61%–80%), spreading distances (0.5 m and 1 m), and observation time (0 min–

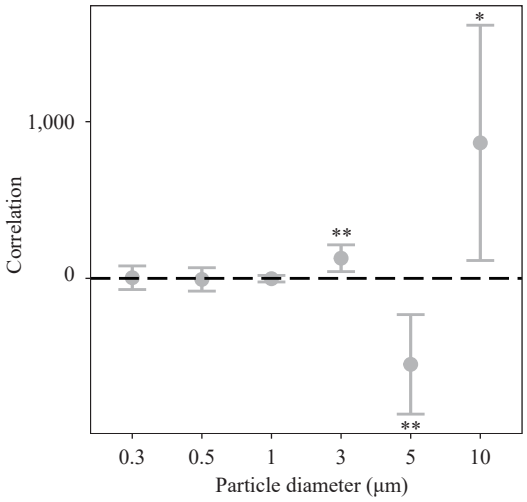

SUPPLEMENTARY FIGURE S1. Effect of the diameters of virus-laden droplets/aerosols on the viral load.
Notes: We defined a correlation greater than 0 as a positive correlation, less than 0 as a negative correlation.
*: significance levels of $P<0.05$.
**: significance levels of $P<0.01$.

120 min). A density plot was used to observe the distribution of viral load as evidence of proper transformation. The intercept of the regression model represented the base status for each environmental factor of interest: time of 0 min, distance of 0.5 m, temperature of 16 ℃–19 ℃, and RH of 30%–45%. Second, we included two-way and three-way interaction terms to account for the interactions amongst the various environmental conditions. Third, we further considered the effects of different particle diameters on the viral load. A *P*-value of 0.05 was taken as the nominal level to determine the statistical significance in all analyses.

REFERENCES

1. Woo MH, Hsu YM, Wu CY, Heimbuch B, Wander J. Method for contamination of filtering facepiece respirators by deposition of MS2 viral aerosols. J Aerosol Sci 2010;41(10):944 – 52. http://dx.doi.org/10.1016/j.jaerosci.2010.07.003.
2. Li X, Ding P, Deng FC, Mao YZ, Zhou L, Ding C, et al. Wearing time and respiratory volume affect the filtration efficiency of masks against aerosols at different sizes. Environ Technol Innov 2022;25:102165. http://dx.doi.org/10.1016/j.eti.2021.102165.
3. Tang S, Li X, Ding P, Mao YX, Deng FC, Cha Y, et al. Filtration efficiency of face masks against aerosolized surrogate SARS-CoV-2 at different social distances. Sci Bull 2022;67(6):565 – 8. http://dx.doi.org/10.1016/j.scib.2021.12.017.

Vital Surveillances

Interactive Effects Between Temperature and $PM_{2.5}$ on Mortality: A Study of Varying Coefficient Distributed Lag Model — Guangzhou, Guangdong Province, China, 2013–2020

Sujuan Chen[1,&]; Hang Dong[2,&]; Mengmeng Li[3]; Lin Huang[1]; Guozhen Lin[2,#]; Qiyong Liu[4]; Boguang Wang[1]; Jun Yang[5,#]

ABSTRACT

Introduction: There is a large body of epidemiological evidence showing significantly increased mortality risks from air pollution and temperature. However, findings on the modification of the association between air pollution and mortality by temperature are mixed.

Methods: We used a varying coefficient distributed lag model to assess the complex interplay between air temperature and $PM_{2.5}$ on daily mortality in Guangzhou City from 2013 to 2020, with the aim of establishing the $PM_{2.5}$-mortality association at different temperatures and exploring synergetic mortality risks from $PM_{2.5}$ and temperature on vulnerable populations.

Results: We observed near-linear concentration-response associations between $PM_{2.5}$ and mortality across different temperature levels. Each 10 μg/m³ increase of $PM_{2.5}$ in low, medium, and high temperature strata was associated with increments of 0.73% [95% confidence interval (CI): 0.38%, 1.09%], 0.12% (95% CI: −0.27%, 0.52%), and 0.46% (95% CI: 0.11%, 0.81%) in non-accidental mortality, with a statistically significant difference between low and medium temperatures (P=0.02). There were significant modification effects of $PM_{2.5}$ by low temperature for cardiovascular mortality and among individuals 75 years or older.

Conclusions: Low temperatures may exacerbate physiological responses to short-term $PM_{2.5}$ exposure in Guangzhou, China.

INTRODUCTION

Ambient air pollution and temperature are leading environmental challenges to global public health. In 2019, $PM_{2.5}$ was responsible for an estimated 4.14 million deaths and 118 million disability-adjusted life years (DALYs) (*1*). Temperature is an important predictor of many diseases and has been perceived as a key environmental factor in climate change scenarios (*2*). Air pollution was identified as the fourth leading risk factor for death worldwide (*3*). Short-term exposure to $PM_{2.5}$ can increase the risk of death from chronic diseases (*4*).

In the context of climate change, health risk assessment of the joint effect of air pollution and temperature has attracted growing public concern (*5*). In Chengdu, China for example, stronger associations between air pollution and hospital admission for chronic obstructive pulmonary disease (COPD) were found at low-temperatures than at moderate temperatures (*6*). However, other studies have failed to identify synergetic health effects of air pollution and temperature. For example, Jhun and co-authors found that the interaction between ozone and temperature was not statistically significant in 97 US cities (*7*). In addition, potential variations of exposure-response patterns under various temperature levels have been less well documented. As an extension of distributed lag models, the varying-coefficient distributed lag model has been flexibly applied to explore interactive and time-lagged effects between different exposure hazards (*8*).

We aimed to establish the exposure-response association between $PM_{2.5}$ and mortality at different temperature strata using the varying coefficient distributed lag model in Guangzhou, China, and to explore synergetic mortality risks from $PM_{2.5}$ and temperature on vulnerable populations.

METHODS

The study period was 2013–2020. We obtained daily mortality data in Guangzhou from Guangzhou Center for Disease Control and Prevention. Causes of death were classified according to International

Classification of Diseases, Tenth Revision: non-accidental causes (A00–R99), cardiovascular disease (I00–I99), ischemic heart disease (IHD, I20–I25), stroke (I60–I69), respiratory disease (J00–J98), and COPD (J40–J47). Daily counts of non-accidental deaths were stratified by age (<75 and ≥75 years), gender, and educational level (≤9 and >9 years). We obtained daily concentrations of air pollutants (O_3, $PM_{2.5}$, PM_{10}, NO_2, SO_2, and CO) from Guangzhou monitoring stations and daily meteorological data from basic weather stations in Guangzhou from the China Meteorological Data Service Center (http://data.cma.cn/).

The varying coefficient distributed lag model, based on generalized linear models with a quasi-Poisson family (*9*), was used to estimate the modifying effect of temperature on the association between $PM_{2.5}$ and mortality. We incorporated several covariates in the model: a natural cubic spline with 7 degrees of freedom (df) per year for a time variable; a natural cubic spline with 3 df for relative humidity, air pressure, and moving average temperature (with time lags of 0–10 days); and holidays and day of the week as indicator variables. The cross-product of categorical temperature levels [low (<25th percentile), medium (25th–75th), and high (>75th percentile)] and $PM_{2.5}$ was used to examine the interaction between air pollution and temperature. In addition, stratified analyses were conducted by gender, age group, and education. Relative differences of RRs across strata [relative risk ratios (*RRR*)] were calculated to detect potential effect modifications by temperature. To verify the robustness of our results, we performed a series of sensitivity analyses. Details of the model are provided in the Supplementary Material (available in https://weekly.chinacdc.cn/). All statistical analyses were conducted in the R language environment (R Core Team 2021, Vienna, Austria) using the "dlnm", "mgcv", and "splines" packages.

RESULTS

Table 1 depicts summary statistics on daily air pollution, weather conditions, and mortality. The average $PM_{2.5}$ value was 35.1 μg/m^3 during 2013–2020. During the study period, there were 403,492 deaths registered in Guangzhou, among which cardiovascular diseases, IHD, stroke, respiratory disease, and COPD accounted for 39.5%, 16.7%, 10.3%, 14.4%, and 6.1%, respectively.

Supplementary Figure S1 (available in https://weekly.chinacdc.cn/) shows Spearman's correlations between air pollution and weather conditions. There were negative correlations between temperature and relative humidity and air pollutants (except for O_3) and positive correlations among air pollutants.

Figure 1 shows lag patterns of $PM_{2.5}$ on cause-specific mortality at different temperature levels. Effect

TABLE 1. Summary statistics for daily weather conditions, air pollution, and mortality in Guangzhou, 2013–2018.

Variable	Mean	Minimum	Percentiles			Maximum
			25th	50th	75th	
Temperature (℃)	22.2	3.4	17.4	23.3	27.3	32.0
Low (<25th)	13.6	4.6	11.8	14.0	15.8	17.7
Medium (25th–75th)	23.1	17.8	20.7	23.3	25.7	27.3
High (>75th)	28.9	27.4	27.9	28.8	29 .6	31.9
Mean humidity (%)	80.4	31.0	75.0	81.5	88.0	100.0
Mean pressure (hPa)	1,007.1	985.7	1,000.3	1,005.4	1,010.8	3,276.6
$PM_{2.5}$ (μg/m³)	35.1	3.5	20.0	30.0	45.0	150.0
Cause (Number of deaths per day)						
Non-accidental	131	79	115	128	143	238
Cardiovascular disease	55	21	45	53	62	115
Ischemic heart disease	23	6	18	22	27	51
Stroke	14	0	11	14	17	34
Respiratory disease	20	6	15	19	24	48
COPD	8	0	6	8	11	30

Abbreviation: COPD=chronic obstructive pulmonary disease.

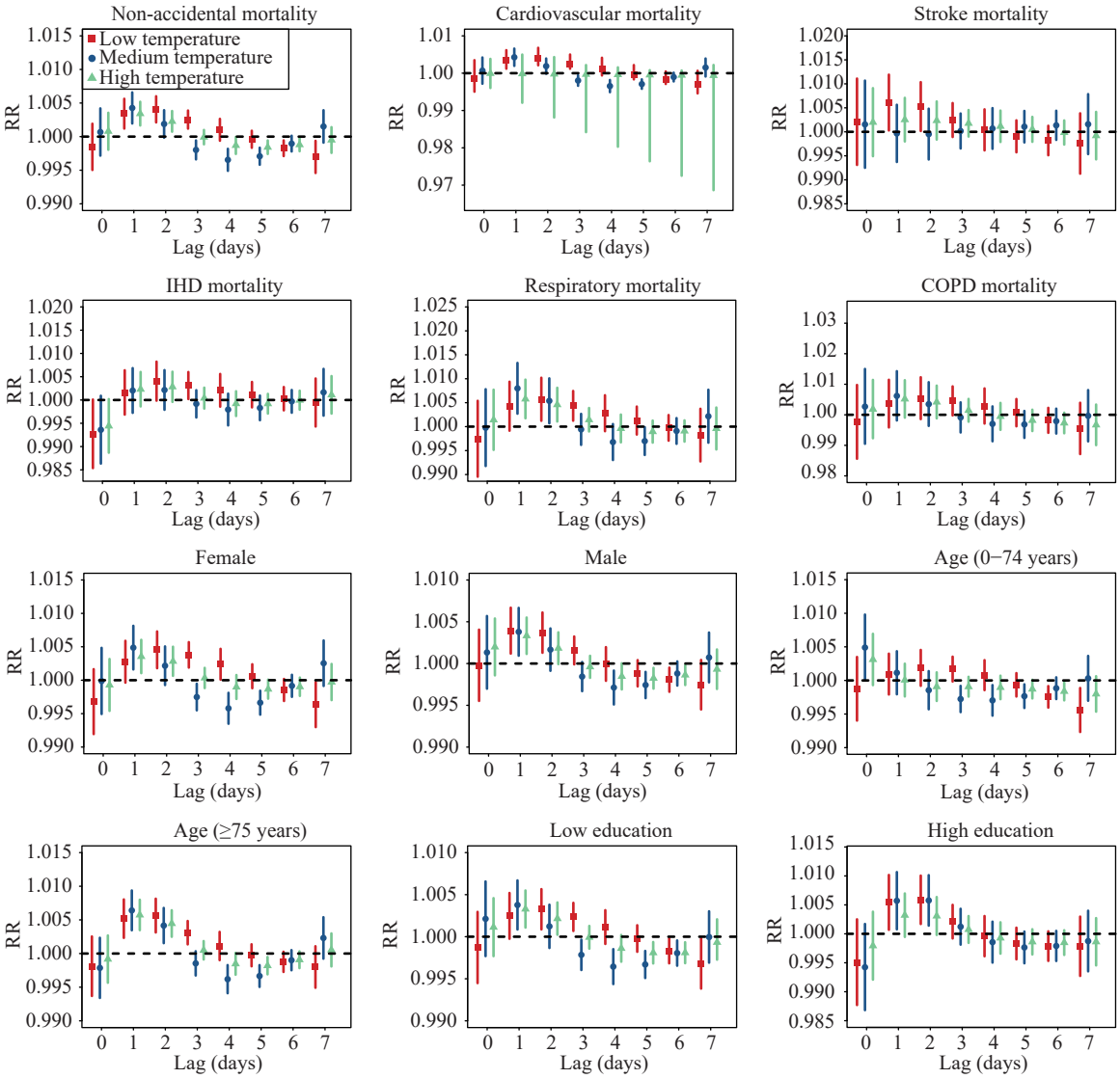

FIGURE 1. RR (95% CI) of mortality associated with 10 μg/m³ increase of $PM_{2.5}$ by a time lag of 0–7 days.
Note: dots and vertical lines represent point estimates and 95% confidence intervals of $PM_{2.5}$ at individual lag days.
Abbreviations: RR=relative risk; IHD=ischemic heart disease; COPD=chronic obstructive pulmonary disease; CI=confidence interval.

of $PM_{2.5}$ on the daily death toll of different diseases had consistent and evident trends in which mortality risks reached maximum within 1–2 lag days of exposure, then leveled off, and disappeared within 4–5 days.

Figure 2 shows the estimates of exposure-response relationships between $PM_{2.5}$ and mortality at different temperature levels. We found approximately linear associations between $PM_{2.5}$ and mortality. The highest effect estimates of $PM_{2.5}$ on mortality were consistently observed at the lower temperatures, while lower effect estimates were seen at the higher temperatures. Each 10 μg/m³ increase of $PM_{2.5}$ in low, medium, and high temperature strata was associated with respective increments of 0.73% [95% confidence interval (CI): 0.38%, 1.09%], 0.12% (95% CI: −0.27%, 0.52%), and 0.46% (95% CI: 0.11%, 0.81%) in non-accidental mortality (Table 2). There was an *RRR* of 1.01 (95% CI: 1.00, 1.01) between low and medium temperatures (*P*=0.02) (Supplementary Table S1, available in https://weekly.chinacdc.cn/). For cause-specific mortality, statistically significant differences between the risk of $PM_{2.5}$ across temperature levels were only observed for cardiovascular mortality, with effect estimates of 0.88% (95% CI: 0.37%, 1.39%), 0.04% (95% CI: −0.52%, 0.60%) and 0.50% (95% CI: 0.00%, 0.99%) at low, medium and high temperature levels (Table 2),

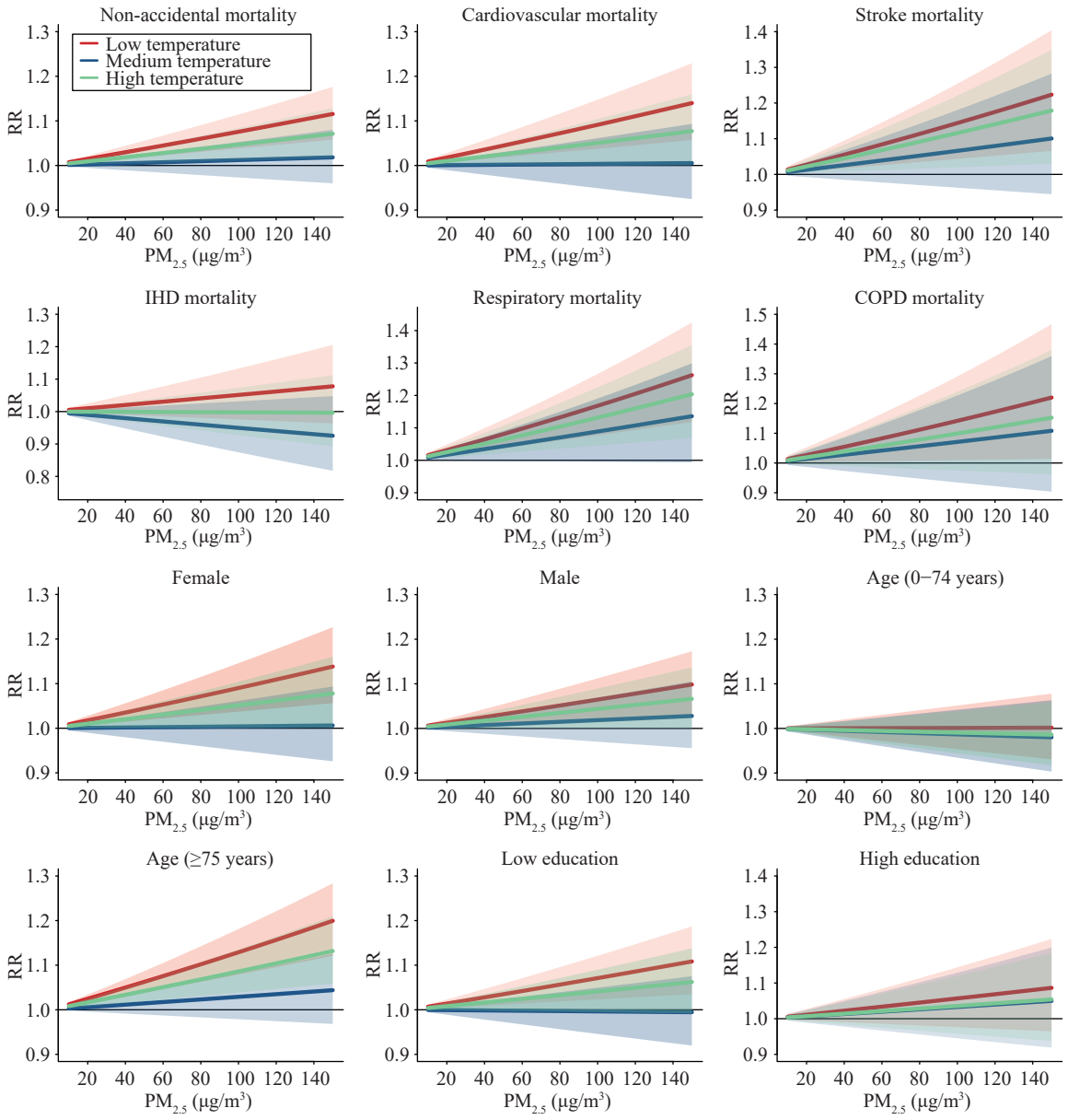

FIGURE 2. Concentration-response associations between $PM_{2.5}$ and mortality under different temperature conditions. Abbreviations: RR=relative risk; IHD=ischemic heart disease; COPD=chronic obstructive pulmonary disease.

and an *RRR* of 1.01 (95% CI: 1.00, 1.02) between low temperature and medium temperature (P=0.03). The highest effect of $PM_{2.5}$ was found in respiratory mortality at low temperatures, with an effect estimate of 1.57% (95% CI: 0.75%, 2.39%); however, difference by temperature was not statistically significant.

In analyses stratified by personal characteristics, we found consistently higher effects of $PM_{2.5}$ at low temperatures compared with medium temperatures, but the only statistically significant difference was among individuals of 75 years or older. Each 10 μg/m³ increase of $PM_{2.5}$ in the low, medium, and high temperature strata was associated with increments of 1.22% (95% CI: 0.76%, 1.68%), 0.29% (95% CI: −0.22%, 0.79%), and 0.83% (95% CI: 0.38%, 1.28%) in mortality of the elderly, respectively, with *RRR* of 1.01 (95% CI: 1.00, 1.02) between low and medium temperature strata (P=0.01). The elderly were more susceptible to $PM_{2.5}$ compared with younger age groups under both low and high temperature conditions.

Using different degrees of freedom for time trend analyses adjusting for co-pollutants changed the effect estimates only slightly (Supplementary Tables S2–S3, available in https://weekly.chinacdc.cn/), indicating

TABLE 2. Cumulative (lag 0–4 days) mortality risk of each 10 μg/m³ increase in $PM_{2.5}$ at different temperature strata (ER, 95% CI).

Variable	Low temperature		Medium temperature		High temperature	
	ER%	95% CI	ER%	95% CI	ER%	95% CI
Non-accidental mortality	0.73*	(0.38, 1.09)*	0.12	(−0.27, 0.52)	0.46*	(0.11, 0.81)*
Cardiovascular mortality	0.88*	(0.37, 1.39)*	0.04	(−0.52, 0.60)	0.50*	(0.00, 0.99)*
Stroke mortality	1.35*	(0.43, 2.29)*	0.64	(−0.38, 1.67)	1.10*	(0.20, 2.02)*
Ischemic heart mortality	0.50	(−0.25, 1.25)	−0.52	(−1.33, 0.31)	−0.02	(−0.64, 0.77)
Respiratory mortality	1.57*	(0.75, 2.39)*	0.85	(−0.04, 1.76)	1.24*	(0.45, 2.05)*
COPD mortality	1.34*	(0.10, 2.59)*	0.69	(−0.67, 2.07)	0.95	(−0.26, 2.17)
Gender						
Female	0.87*	(0.37, 1.37)*	0.04	(−0.51, 0.60)	0.50*	(0.01, 1.00)*
Male	0.63*	(0.19, 1.07)*	0.18	(−0.30, 0.67)	0.43*	(0.00, 0.86)*
Age (years)						
0–74	0.01	(−0.48, 0.50)	−0.13	(−0.68, 0.41)	−0.09	(−0.57, 0.39)
≥75	1.22*	(0.76, 1.68)*	0.29	(−0.22, 0.79)	0.83*	(0.38, 1.28)*
Education						
Low education	0.69*	(0.23, 1.15)*	−0.04	(−0.56, 0.48)	0.40	(−0.05, 0.86)
High education	0.55	(−0.24, 1.35)	0.32	(−0.56, 1.22)	0.32	(−0.43, 1.14)

Abbreviations: ER=excess risk; CI=confidence interval; COPD=chronic obstructive pulmonary disease.
* indicates statistically significant results.

robustness of our main results. Using different temperature cutoffs (Supplementary Table S4, available in https://weekly.chinacdc.cn/) and different $PM_{2.5}$ time-lags (Supplementary Table S5, available in https://weekly.chinacdc.cn/) did not remarkably change the estimates of temperature-stratified air pollution effects on mortality.

CONCLUSIONS

To the best of our knowledge, this is one of the few studies exploring exposure-response associations between air pollution and mortality under different temperature conditions. Our study consistently observed greater mortality risks from $PM_{2.5}$ in lower temperatures than in moderate temperatures across different causes of death. Interaction effects between $PM_{2.5}$ and low temperatures were more pronounced in the elderly than in younger people.

We observed the highest effect of $PM_{2.5}$ on mortality in low temperature strata compared with high and medium temperature strata. Low temperatures have consistently been found to enhance the effect of $PM_{2.5}$ on cardiovascular mortality in Beijing (*10*), natural and respiratory mortality in Hong Kong (*11*), and COPD mortality in Chengdu (*6*). For instance, Li and coauthors found that each 10 μg/m³ increment of $PM_{2.5}$ during the lowest temperature range was associated with a 1.27% (95% CI: 0.38%, 2.17%) increase in cardiovascular mortality, compared with 0.59% (95% CI: 0.22%, 1.16%) across the whole temperature range (*10*). Likewise, the association between $PM_{2.5}$ and mortality in Hong Kong was stronger at low temperatures than at higher temperatures, with corresponding effect estimates of 0.94% (0.95% CI: 0.65%, 1.24%) and 0.47% (95% CI: 0.65%, 1.24%) for each 10 μg/m³ increment in $PM_{2.5}$ (*11*). The reduced beat frequency of nose and trachea cilia on cold days, which affects the clearance rate of particulate matter and makes people more susceptible to $PM_{2.5}$, is suspected as an underlying mechanism for the greater effect of $PM_{2.5}$ on mortality at low temperatures in Guangzhou (*12*). Some studies found that people living in warm regions probably experience a higher mortality risk during cold weather than do people living in cold regions (*13*). In addition, low temperatures may exacerbate airway inflammation and increase the burden on respiratory functions (*14*).

We also found relatively higher effect estimates of $PM_{2.5}$ on mortality in high temperatures compared to moderate temperatures, although the difference was not statistically significant, consistent with previous studies (*6*,*10*). However, another study reported a statistically significant higher health effect of $PM_{2.5}$ in

high temperature strata (*15*). The discrepant results may be explained by differences in population structure and air pollution exposure patterns.

In this study, we observed a significant modification of the effect of $PM_{2.5}$ on cardiovascular mortality by low temperatures. As ambient temperature decreases, cold receptors in the skin are stimulated, the sympathetic nervous system increases catecholamine levels, blood vessels near the skin constrict to reduce heat loss, and blood pressure suddenly increases (*10*). High blood pressure can lead to oxygen deficiency, myocardial ischemia, or arrhythmia, and become a risk factor for vascular spasms and ruptures of atherosclerotic plaque that cause thromboses (*12*). Such marked changes make people more susceptible to adverse cardiovascular outcomes caused by $PM_{2.5}$. The findings are important from a public health perspective, as 39.5% of all non-accidental deaths in Guangzhou were cardiovascular deaths.

Our analysis also found significant interaction effects of $PM_{2.5}$ and low temperature among the elderly but not among young people, which is consistent with a previous study (*6*). The body's homeostasis and thermoregulatory functions, and the capacity to eliminate chemicals from the body decrease with age (*16*), which may contribute to the combined health hazards of $PM_{2.5}$ and temperature change. The elderly also suffer from higher rates of comorbidities, which may further enhance their vulnerability to environmental exposure.

The study was subject to some limitations. First, we substituted measured air pollution and air temperature at fixed outdoor monitoring stations for personal exposures, which will lead to some exposure measurement errors. Second, only adverse associations of $PM_{2.5}$ were examined in this study, leaving confounding by other factors unexplored. Last, our results may not generalize to areas with different population structures and air pollution compositions.

In summary, we observed an interaction between $PM_{2.5}$ and low temperature on mortality, especially for non-accidental and cardiovascular mortality and among the elderly. Considering the synergetic health risks of air pollution and temperature, cooperation from multiple sectors with the aim of protecting vulnerable populations may mitigate health challenges from climate change and air pollution.

Funding: Supported by the National Natural Science Foundation of China (No. 82003552), and the Guangdong Basic and Applied Basic Research Foundation (No. 2020A1515011161, 2021A1515 110625, 2020A1414010168).

doi: 10.46234/ccdcw2022.124

[#] Corresponding authors: Jun Yang, yangjun@gzhmu.edu.cn; Guozhen Lin, xwkgzcdc@126.com.

[1] Institute for Environmental and Climate Research, Jinan University, Guangzhou, Guangdong Province, China; [2] Guangzhou Center for Disease Control and Prevention, Guangzhou, Guangdong Province, China; [3] Department of Cancer Prevention, State Key Laboratory of Oncology in South China, Collaborative Innovation Center for Cancer Medicine, Sun Yat-sen University Cancer Center, Guangzhou, Guangdong Province, China; [4] National Center for Chronic and Noncommunicable Disease Control and Prevention, Beijing, China; [5] School of Public Health, Guangzhou Medical University, Guangzhou, Guangdong Province, China.
[&] Joint first authors.

Submitted: April 16, 2022; Accepted: June 17, 2022

REFERENCES

1. Institute for Health Metrics and Evaluation. Ambient particulate matter pollution — Level 4 risk. https://www.healthdata.org/results/gbd_summaries/2019/ambient-particulate-matter-pollution-level-4-risk. [2022-05-24]
2. Yang J, Zhou MG, Ren ZP, Li MM, Wang BG, Liu DL, et al. Projecting heat-related excess mortality under climate change scenarios in China. Nat Commun 2021;12(1):1039. http://dx.doi.org/10.1038/s41467-021-21305-1.
3. Murray CJL, Aravkin AY, Zheng P, Abbafati C, Abbas KM, Abbasi-Kangevari M, et al. Global burden of 87 risk factors in 204 countries and territories, 1990–2019: a systematic analysis for the Global Burden of Disease Study 2019. Lancet 2020;396(10258):1223 – 49. http://dx.doi.org/10.1016/S0140-6736(20)30752-2.
4. Cheng H, Zhu FR, Lei RQ, Shen CW, Liu J, Yang M, et al. Associations of ambient $PM_{2.5}$ and O_3 with cardiovascular mortality: a time-series study in Hefei, China. Int J Biometeorol 2019;63(10):1437 – 47. http://dx.doi.org/10.1007/s00484-019-01766-2.
5. Li J, Woodward A, Hou XY, Zhu T, Zhang JL, Brown H, et al. Modification of the effects of air pollutants on mortality by temperature: a systematic review and meta-analysis. Sci Total Environ 2017;575:1556 – 70. http://dx.doi.org/10.1016/j.scitotenv.2016.10.070.
6. Qiu H, Tan K, Long FY, Wang LY, Yu HY, Deng R, et al. The burden of COPD morbidity attributable to the interaction between ambient air pollution and temperature in Chengdu, China. Int J Environ ResPublic Health 2018;15(3):492. http://dx.doi.org/10.3390/ijerph15030492.
7. Jhun I, Fann N, Zanobetti A, Hubbell B. Effect modification of ozone-related mortality risks by temperature in 97 US cities. Environ Int 2014;73:128 – 34. http://dx.doi.org/10.1016/j.envint.2014.07.009.
8. Zhao X, Chen F, Feng ZJ, Li XS, Zhou XH. Characterizing the effect of temperature fluctuation on the incidence of malaria: an epidemiological study in south-west China using the varying coefficient distributed lag non-linear model. Malar J 2014;13:192. http://dx.doi.org/10.1186/1475-2875-13-192.
9. Gasparrini A, Guo YM, Hashizume M, Kinney PL, Petkova EP, Lavigne E, et al. Temporal variation in heat-mortality associations: a multicountry study. Environ Health Perspect 2015;123(11):1200 – 7. http://dx.doi.org/10.1289/ehp.1409070.
10. Li Y, Ma ZQ, Zheng CJ, Shang Y. Ambient temperature enhanced acute cardiovascular-respiratory mortality effects of $PM_{2.5}$ in Beijing, China. Int J Biometeorol 2015;59(12):1761 – 70. http://dx.doi.org/10.1007/s00484-015-0984-z.
11. Sun SZ, Cao PH, Chan KP, Tsang H, Wong CM, Thach TQ. Temperature as a modifier of the effects of fine particulate matter on

acute mortality in Hong Kong. Environ Pollut 2015;205:357 – 64. http://dx.doi.org/10.1016/j.envpol.2015.06.007.
12. Jiang YX, Chen RJ, Kan HD. The interaction of ambient temperature and air pollution in China. In: Lin HL, Ma WJ, Liu QY, editors. Ambient temperature and health. Singapore: Springer. 2019105 – 16. http://dx.doi.org/10.1007/978-981-13-2583-0_7.
13. Yang J, Yin P, Zhou MG, Ou CQ, Guo YM, Gasparrini A, et al. Cardiovascular mortality risk attributable to ambient temperature in China. Heart 2015;101(24):1966 – 72. http://dx.doi.org/10.1136/heartjnl-2015-308062.
14. Deng LJ, Ma P, Wu Y, Ma YS, Yang X, Li YG, et al. High and low temperatures aggravate airway inflammation of asthma: evidence in a mouse model. Environ Pollut 2020;256:113433. http://dx.doi.org/10.1016/j.envpol.2019.113433.
15. Qian ZM, He QC, Lin HM, Kong LL, Bentley CM, Liu WS, et al. High temperatures enhanced acute mortality effects of ambient particle pollution in the "oven" city of Wuhan, China. Environ Health Perspect 2008;116(9):1172 – 8. http://dx.doi.org/10.1289/ehp.10847.
16. Simoni M, Baldacci S, Maio S, Cerrai S, Sarno G, Viegi G. Adverse effects of outdoor pollution in the elderly. J Thorac Dis 2015;7(1):34 – 45. http://dx.doi.org/10.3978/j.issn.2072-1439.2014.12.10.

SUPPLEMENTARY MATERIAL

Model Construction

The varying coefficient distributed lag model:

$$Log[E(Y_t)] = \alpha + ns(Hum_t, 3) + ns(Press_t, 3) + ns(Temp_t, 3) + ns(Time_t, 78) + \upsilon Holiday_t + cb(PM_{2.5}) + T_l \times cb(PM_{2.5})$$

Where $E(Y_t)$ denotes the daily expected number of deaths on day t; α is the intercept; ns is a natural cubic spline. 7 degrees of freedom (df) per year for time ($Time_t$) was used to control for long-term trends and seasonal variables of daily mortality (*1*). $Holiday_t$ is an indicator variable of population dynamics due to holidays. T_l is a categorical variable indicating various temperature levels. To explore the possible effect modification by ambient temperature, we divided the ambient temperature into three levels: low (<25th percentile), medium (25th–75th), and high (>75th percentile), which was consistent with previous studies (*2*). ns (natural cubic splines) with three df was adapted for daily relative humidity and air pressure (*3*). And we applied the natural cubic spline (ns) to fit the moving average (lag 0–10 days) of temperature to control the confounding effects of temperature ($Temp_t$). In the basic model, we used a distributed lag model (DLM) to describe the association with $PM_{2.5}$. Lag effects were described by a cross-basis function (cb) in the distributed lag model (*4*). Specifically, we applied a cross-basis

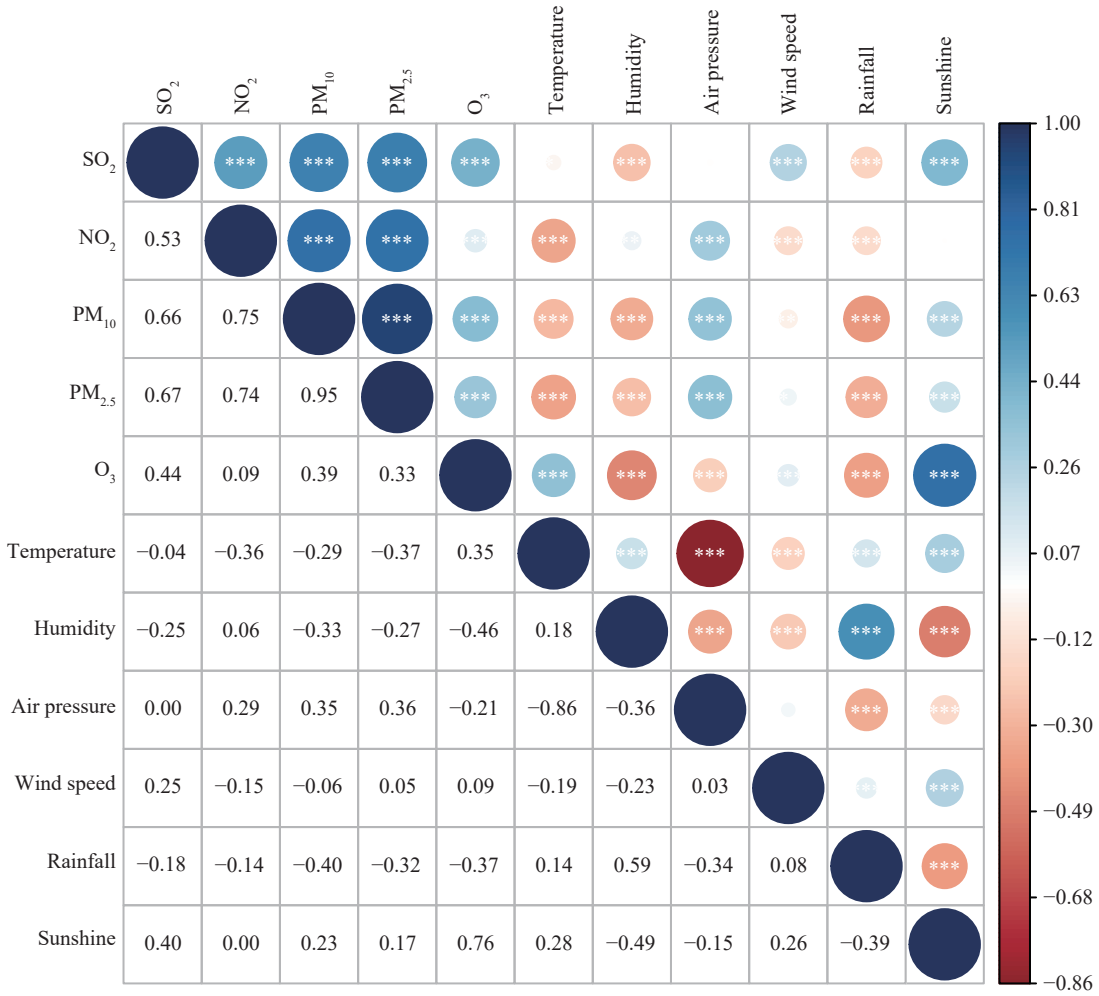

SUPPLEMENTARY FIGURE S1. Correlations (Spearman correlation coefficient) among air pollution and weather conditions.
*: P<0.05;
**: P<0.01;
***: P<0.001.

SUPPLEMENTARY TABLE S1. *RRR*, 95% confidence intervals (CI), and *P*-values of significance test of effects of $PM_{2.5}$ (per 10 μg/m^3) on mortality under different temperature levels.

Variable	Medium temperature	Low temperature			High temperature		
		RRR	95% CI	*P*	*RRR*	95% CI	*P*
Cause							
Non-accidental mortality	Reference	1.006*	(1.001, 1.011)*	0.024*	1.003	(0.998, 1.009)	0.207
Cardiovascular mortality	Reference	1.008*	(1.001, 1.016)*	0.030*	1.005	(0.997, 1.012)	0.228
Stroke mortality	Reference	1.007	(0.993, 1.021)	0.315	1.005	(0.991, 1.018)	0.511
IHD mortality	Reference	1.010	(0.999, 1.022)	0.072	1.005	(0.994, 1.016)	0.365
Respiratory mortality	Reference	1.007	(0.995, 1.019)	0.247	1.004	(0.992, 1.016)	0.526
COPD mortality	Reference	1.006	(0.99, 1.023)	0.434	1.003	(0.987, 1.019)	0.751
Gender							
Female	Reference	1.005	(0.997, 1.012)	0.219	1.001	(0.994, 1.008)	0.793
Male	Reference	1.004	(0.998, 1.011)	0.178	1.002	(0.996, 1.009)	0.450
Age (years)							
0–74	Reference	1.001	(0.994, 1.009)	0.708	1.000	(0.993, 1.008)	0.914
≥75	Reference	1.009*	(1.002, 1.016)*	0.008*	1.005	(0.999, 1.012)	0.118
Education level							
Low education	Reference	1.007	(0.997, 1.017)	0.153	1.004	(0.997, 1.011)	0.212
High education	Reference	1.002	(0.991, 1.014)	0.698	1.000	(0.988, 1.012)	1.000

Abbreviations: *RRR*=relative risk ratios; IHD=ischemic heart disease; COPD=chronic obstructive pulmonary disease.
* indicate statistically significant results.

SUPPLEMENTARY TABLE S2. Sensitivity analysis of the modification by the temperature on the $PM_{2.5}$-mortality association using 5–8 degrees of freedom (df) per year for the time trend.

Degrees of freedom (df)	Low temperature		Medium temperature		High temperature	
	ER	95% CI	ER	95% CI	ER	95% CI
df=6	0.73	(0.38, 1.09)	0.12	(−0.27, 0.52)	0.46	(0.11, 0.81)
df=5	0.81	(0.46, 1.16)	0.17	(−0.21, 0.54)	0.49	(0.15, 0.83)
df=7	0.68	(0.32, 1.04)	0.11	(−0.29, 0.51)	0.39	(0.03, 0.75)
df=8	0.74	(0.38, 1.10)	0.20	(−0.19, 0.60)	0.46	(0.11, 0.82)

Abbreviations: ER=excess risk; CI=confidence interval.

SUPPLEMENTARY TABLE S3. Sensitivity analysis of the modification by the temperature on the air pollution-mortality association with adjustments for different co-pollutants.

Co-pollutants	Low temperature		Medium temperature		High temperature	
	ER	95% CI	ER	95% CI	ER	95% CI
Main model	0.73	(0.38, 1.09)	0.12	(−0.27, 0.52)	0.46	(0.11, 0.81)
$PM_{2.5}$ + SO_2	0.41	(−0.01, 0.84)	−0.19	(−0.65, 0.27)	0.14	(−0.28, 0.56)
$PM_{2.5}$ + NO_2	0.86	(0.42, 1.31)	0.24	(−0.23, 0.71)	0.53	(0.09, 0.97)
$PM_{2.5}$ + O_3	0.59	(0.21, 0.97)	−0.04	(−0.46, 0.38)	0.33	(−0.05, 0.71)

Abbreviations: ER=excess risk; CI=confidence interval.

composed of a linear function for exposure-response, and a natural cubic B-spline for the lag response with an intercept and two internal knots placed at equally spaced values in the log scale. We chose 4 days to examine the lag effect of $PM_{2.5}$.

In this study, we extended distributed lag model (DLM) to the varying coefficient DLM by including a linear interaction between temperature (T_l) and the cross-basis variables. We directly incorporated the principal and

SUPPLEMENTARY TABLE S4. Sensitivity analysis of the modification by the temperature on the $PM_{2.5}$-mortality association using different temperature cutoffs.

Temperature cutoffs	Low temperature		Medium temperature		High temperature	
	ER	95% CI	ER	95% CI	ER	95% CI
25th/75th	0.73	(0.38, 1.09)	0.12	(−0.27, 0.52)	0.46	(0.11, 0.81)
20th/80th	0.61	(0.26, 0.96)	0.20	(−0.21, 0.60)	0.45	(0.10, 0.80)
15th/85th	0.51	(0.16, 0.86)	0.46	(0.02, 0.89)	0.45	(0.10, 0.80)
10th/90th	0.50	(0.14, 0.85)	0.73	(0.26, 1.21)	0.44	(0.09, 0.79)

Abbreviations: ER=excess risk; CI=confidence interval.

SUPPLEMENTARY TABLE S5. Sensitivity analysis of the modification by the temperature on the $PM_{2.5}$-mortality association using different days of lag.

Days of lag	Low temperature		Medium temperature		High temperature	
	ER	95% CI	ER	95% CI	ER	95% CI
Lag 0–4	0.73	(0.38, 1.09)	0.12	(−0.27, 0.52)	0.46	(0.11, 0.81)
Lag 0–3	0.81	(0.48, 1.15)	0.24	(−0.14, 0.61)	0.57	(0.24, 0.89)
Lag 0–5	0.56	(0.19, 0.94)	−0.05	(−0.46, 0.37)	0.29	(−0.08, 0.66)
Lag 0–6	0.43	(0.03, 0.83)	−0.15	(−0.58, 0.28)	0.17	(−0.22, 0.56)

Abbreviations: ER=excess risk; CI=confidence interval.

interaction terms in the model during a special parameterization to satisfy the DLM software specifications. The interaction term, the cross-product of the categorical temperature variable and $PM_{2.5}$ were used to examine the interaction effects between air pollution and temperature. We can estimate the effects of air pollution at a specific temperature from the three-dimensional curve. For instance, to obtain the effect of temperature at the specific concentration of air pollution, we only need to provide 3 coefficients of unidimensional NS splines that modeled the overall cumulative exposure-response relationship. Further, with the temperature divided into three levels, the model specifications and interpretations were similar. We then used this varying coefficient DLM to predict the exposure-lag-response association for different temperature strata. To examine potentially vulnerable populations, we repeated statistical analyses by gender, age group, and education to examine the changes in effect estimates across subgroups.

In order to detect the potential effect modifications of temperature, we calculated the relative differences of RRs across strata [relative risk ratio (*RRR*)] with the following equation.

$$RRR = exp\left[(E_1 - E_2) \pm 1.96\sqrt{SE_1^2 + SE_2^2}\right]$$

where E_1 and E_2 denote the effect estimates [i.e. ln(RR)] of two subgroups; $SE(E_1)$ and $SE(E_2)$ are corresponding standard errors of E_1 and E_2 (*5*).

REFERENCES

1. Li L, Yang J, Guo C, Chen PY, Ou CQ, Guo YM. Particulate matter modifies the magnitude and time course of the non-linear temperature-mortality association. Environ Pollut 2015;196:423 – 30. http://dx.doi.org/10.1016/j.envpol.2014.11.005.
2. Chen K, Wolf K, Breitner S, Gasparrini A, Stafoggia M, Samoli E, et al. Two-way effect modifications of air pollution and air temperature on total natural and cardiovascular mortality in eight European urban areas. Environ Int 2018;116:186 – 96. http://dx.doi.org/10.1016/j.envint.2018.04.021.
3. Yang Z, Yang J, Zhou MG, Yin P, Chen ZY, Zhao Q, et al. Hourly temperature variability and mortality in 31 major Chinese cities: effect modification by individual characteristics, season and temperature zone. Environ Int 2021;156:106746. http://dx.doi.org/10.1016/j.envint.2021.106746.
4. Gasparrini A. Modeling exposure-lag-response associations with distributed lag non-linear models. Stat Med 2014;33(5):881 – 99. http://dx.doi.org/10.1002/sim.5963.
5. Yang J, Yin P, Sun JM, Wang BG, Zhou MG, Li MM, et al. Heatwave and mortality in 31 major Chinese cities: definition, vulnerability and implications. Sci Total Environ 2019;649:695 – 702. http://dx.doi.org/10.1016/j.scitotenv.2018.08.332.

Review

Air Pollution Health Impact Monitoring and Health Risk Assessment Technology and Its Application — China, 2006–2019

Jingxiu Han[1]; Dongqun Xu[1,#]; Donggang Xu[2]; Xu Yang[3]; Qin Wang[1]; Mingqing Chen[3]; Wenrong Xia[2]; Weiwei Xing[2]; Chunyu Xu[1]; Yue Liu[1]; Junrui Chang[1]; Wenliang Fu[2]; Shuxin Hao[1]; Na Li[1]; Xiaoyan Dong[1]; Yunpu Li[1]; Congshen Meng[1]; Jingyi Liu[1]

ABSTRACT

Air pollution is a significant risk factor contributing to the burden of disease in China. Health risk assessment and management are important to reduce the impact of air pollution on public health. To help formulate standardized health risk assessment techniques, a series of studies were conducted from 2006 to 2019. Through systematic review, study of molecular mechanisms, epidemiological investigation, and health effect monitoring, the overall project established a monitoring and evaluation indicator system, a comprehensive information platform, software for automatic data cleaning, and standardized health risk assessment techniques. Technical specifications have been issued by the National Health Commission for promoting health risk assessments across China. This paper introduces the project, the research approach, its main research accomplishments, innovations, and public health significance, and describes directions for further research.

BACKGROUND

Air pollution is one of the most important public health problems in China. The Global Burden of Disease Study found that ambient and household air pollution were the fourth and fifth most significant risk factors contributing to the nation's age-standardized disability-adjusted life-years rating (*1*). To reduce the impact of air pollution on health, China enacted laws requiring the establishment and improvement of environment and health monitoring, investigations, and risk assessment systems. Establishing a comprehensive air pollution and health monitoring system and health risk assessment technology involved three major technical problems. First, a population-wide indicator system for monitoring and evaluating the health effects of air pollution that spanned the life cycle and range of severity, from sub-clinical health effects to death, needed to be established. Second, a comprehensive information platform that incorporated multi-source data integration and data quality control was required. Third, a health risk assessment technology needed to be established based on the mechanisms of action of air pollution on health.

After 14 years of hard work, a multi-disciplinary collaborative research program was finished ,which was funded by the National Health Commission (NHC), the Ministry of Science and Technology, and the National Natural Science Foundation of China. Through a series of studies (systematic reviews, molecular mechanisms studies, epidemiological investigations, and health effect monitoring), the three major technical problems were solved, and specifications were formulated. The project identified the major health impacts and potential health risks of urban air pollution and is working to reduce disease burden by integrating health into air pollution prevention and control policies.

OVERALL RESEARCH APPROACH

Figure 1 shows the studies used to establish a monitoring and evaluation indicator system (MEIS), a comprehensive information platform, and health risk assessment technology. First, MEIS indicators (i.e., air pollution, and health influencing factors) were established through systematic literature review, mechanistic studies of respiratory system damage and cardiovascular disease, and analyses of existing air pollution and health monitoring systems.

Second, air quality, meteorological, toxicological, and health data were collected in selected cities with smog. After analyzing the data, evaluating data quality, and defining a data dictionary, an information

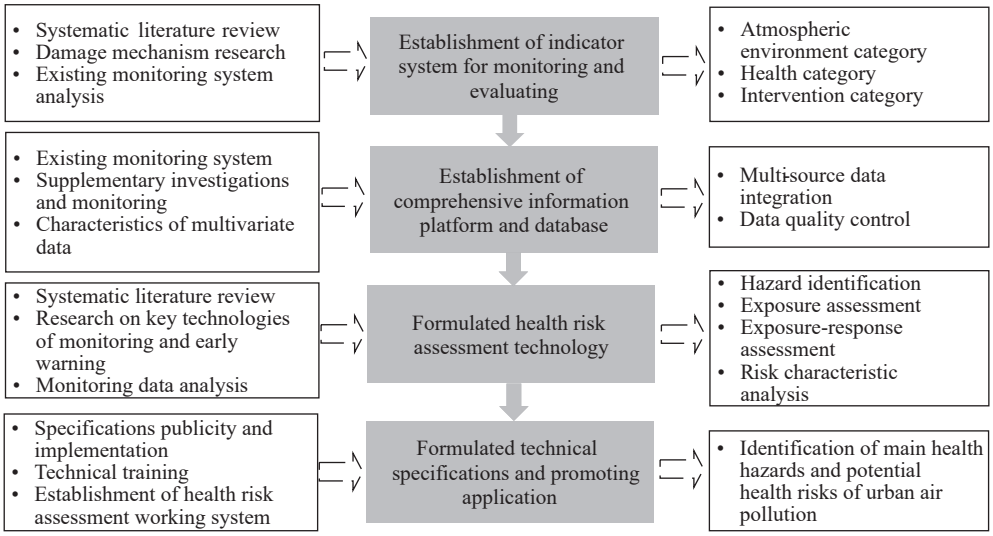

FIGURE 1. Overall research approach of air pollution health impact monitoring and health risk assessment technology and its application.

platform and database for integrated monitoring of air pollution on health was established.

Third, data application rules were clarified by studying relevant technologies, after which accurate exposure assessment models, exposure-response assessment models, public health risk assessment models, and health risk assessment techniques for air pollution were established. Finally, the indicator system, a comprehensive information platform, and health risk assessment technology were promoted to provide technical support for establishing and improving the health risk assessment system and implementing health risk management.

RESEARCH ACCOMPLISHMENTS

Figure 2 shows the research milestones leading to the indicator system, the information platforms and database, and health risk assessment technology.

Indicator System

In accordance with the World Health Organization (WHO) Driving Force-Pressure-State-Exposure-Effect-Action (DPSEEA) framework and the American hazard, exposure, health effects, and intervention (HEHI) framework, air pollution and health indicators were divided into basic, atmospheric environment, health, and intervention categories (*2*). Indicators with clear and probable causal evidence for health effects were stratified into core indicators. Research clarified the health impact of indicators that are closely related to or possibly have causal effects on health.

A guiding principle was that the indicator set should make full use of existing monitoring data in China. Studies were conducted in eight cities to determine the relationship between smog pollutant characteristics and health. Disease and death data were obtained from existing monitoring or registration systems, and data characteristics, quality, accessibility, and availability were evaluated. Ultimately, an atmospheric pollution environmental health indicator system was established based on existing literature, mechanism studies, and data from existing monitoring systems (*2*).

Information Platform and Database

Data from existing monitoring systems and supplementary investigations were used to establish a comprehensive information platform and database in selected cities with smog. Relevant data included air pollutant and fine particulate matter ($PM_{2.5}$) composition, meteorological factors, and multi-sourced data on physiological and functional indicators for entire populations and sub-groups — morbidity and symptoms, hospital outpatient services, emergencies, and hospitalizations, and causes of death. Multivariate analyses were conducted, and a data dictionary was defined. A basic database on health impact of smog was established, and data rules were defined. Data quality was evaluated by assessing repeatability, completeness, validity, and standardization. An object-oriented methodology was used to design the software, and the resulting Comprehensive Information Platform for Health Impact of Smog (HIS platform) was developed in Java with middleware technology and centralized

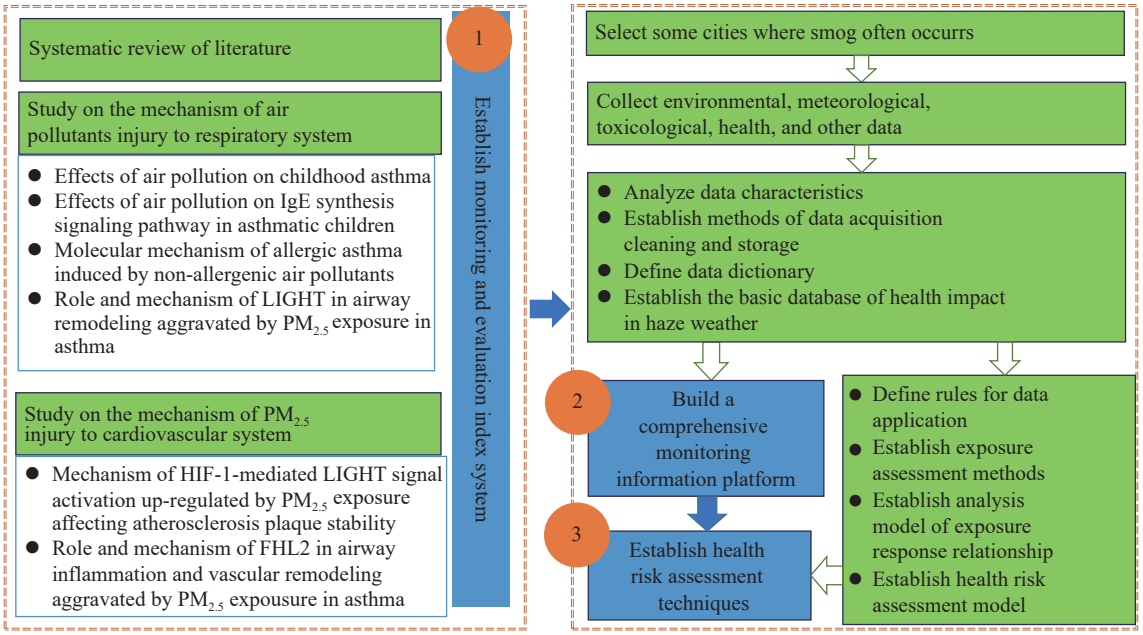

FIGURE 2. Research milestones of air pollution health impact monitoring and health risk assessment technology and its application.
Abbreviation: LIGHT=Tumor necrosis factor ligand superfamily member 14, a tumor necrosis factor (TNF) superfamily ligand; IgE=Immunoglobulin E; HIF-1= hypoxia inducible factor-1; FHL2=four and a half LIM domain protein 2.

data management. This approach allowed for multi-source data collection, data quality assessment, statistical analyses, data management, and visual display of analytic results.

Automated Data Cleaning Tools

Java was used to develop the Toolkit Software for Cleaning Monitoring Data of Air Pollutants and Health (CMDAPH software) in a structured query language database. The resulting software is a secure tool without requiring installation. It is easy to operate, allowing for intuitive data import, automatic auditing, cleaning, export, and visual display. A professional book was published: "*Methods for Data Cleaning and Public Health Impact Evaluation of Air Pollutant.*"

Health Risk Assessment and Technical Specifications

Health hazards were identified through a systematic literature review and the findings of molecular mechanism studies of airway and blood vessel damage due to typical air pollutants. An accurate assessment model of individual exposure to $PM_{2.5}$ was established by integrating air pollution data, building characteristics, permeability coefficients, 24-hour population activity patterns, and concentrations of air pollutants in microenvironments. Exposure-response evaluation models suitable for long-term or short-term exposure were formulated using public health, air pollution, and meteorological data. Based on sensitivity analyses, the influence of other air pollutants, meteorological factors, day of the week, time, and seasonal trends were adjusted to evaluate the relation between smog exposure and outcomes in several pilot cities in China. This model became a key method for population-based and toxicity-based health risk assessments. These technologies were integrated to develop comprehensive, mechanistic health risk assessments. Major project outputs included the publication of the *Methods and Application for Health Risk Assessment of Air Pollution*, and formulation of *Technical Specifications for Health Risk Assessment of Ambient Air Pollution* (HRAAAP specification, WS/T 666–2019).

INNOVATIONS

This project brought about several technical innovations in systems integration. Based on molecular mechanism study results, monitoring data analyses, and DPSEEA and HEHI frameworks, an end-to-end technology system was established. This system, in turn, led to the establishment of a monitoring and evaluation indicator system, a comprehensive information platform with multi-source data

integration and data quality control, and comprehensive health risk assessment technology.

The molecular mechanism studies yielded six major findings or outputs. First, non-allergenic air pollutants such as formaldehyde, phthalate, and $PM_{2.5,}$ may cause allergies and asthma. Second, two phthalates (i.e., diisononyl phthalate, Di 2-Ethyl Hexyl Phthalate (DEHP)] increase blood pressure by activating angiotensin converting enzyme and inhibiting the nitric oxide (NO) pathway. DEHP with high molecular weight and dibutyl phthalate with low molecular weight had different effects on blood pressure due to their differential effects on the renin-angiotensin-aldosterone system or estrogen levels (*3*–*6*). Third, $PM_{2.5}$ exposure can induce the expression of nitric oxide synthase 2 (NOS2) and production of NO to cause high levels of autophagy. Conversely, blocking the NOS2 signaling pathway can inhibit autophagosome formation and subsequent cell death. NO plays a key role in the lung oxidative stress response earlier than in inflammatory responses (*7*). Fourth, four and a half LIM domain protein 2 (FHL2) and autophagy play an important role in the vascular inflammatory response and vascular remodeling induced by $PM_{2.5}$ exposure (*8*). Fifth and sixth, two markers and primers developed in this project were converted to patents — a marker for the detection of asthma in children (Grant No. ZL 201110060515.7) and a marker and primer for the detection of asthma in children (Grant No. ZL 201310299330.0).

Another innovative development is obtaining software copyrights by the project's HIS platform and CMDAPH software.

The $PM_{2.5}$ individual exposure assessment model became more accurate and comprehensive, as it considered building characteristics, indoor and outdoor $PM_{2.5}$ concentrations, permeability coefficients, 24-hour population activity characteristics, and the concentrations of air pollutants in residential, office, supermarket, outdoor exercise, or transportation settings (*9*–*10*).

Finally, the HRAAAP specification represented the first health risk assessment standard of environmental exposure for China's health industry (*11*).

PUBLIC HEALTH SIGNIFICANCE

The key air pollution health risk assessment technologies established by the project expanded the understanding of health impacts and health risks caused by typical air pollutants and provided technical support for establishing an environmental health risk assessment and risk management system.

Promoting Monitoring and Health Risk Assessment Across the Country

Due to severe smog and concerns about its health impact, NHC launched the national air pollution (smog) health impact monitoring program in 2013. The establishment of a timely indicator system provided a top-level design and monitoring scheme. The HIS platform and CMDAPH software have also been widely used in monitoring projects since 2017, including in applications in all 31 provincial-level administrative divisions (PLADs), 87 monitoring cities, and 167 monitoring sites by 2021.

The HRAAAP specification was promulgated by NHC in 2019 and officially implemented on January 1, 2020. By implementing standardized technical training in the monitoring program, monitoring staff in the 31 PLADs improved their skills in data review, clearing, statistical analysis, and health risk assessment. Air pollution health risk assessment has been widely implemented in monitoring cities. Identification of major health impacts and potential health risks of urban air pollution based on local conditions provides evidence and a scientific basis for the formulation of air pollution prevention and control policies and the development of targeted health protection measures.

Decision-making Basis for National Environmental Health Actions

Promulgation and implementation of the HRAAAP specification enabled the establishment of relevant standards for environmental and health risk assessment and laid a foundation for establishing a risk assessment system. It also supported decision-making related to air pollution health risk management and public health protection in China. Relevant results provided a scientific basis for formulating the Three-year Action Plan for Resolutely Fighting the Battle Against Pollution, Comprehensively Strengthening Environmental and Health Work, and the Healthy China Action (2019–2030): Action to Promote a Healthy Environment.

Enhancing Public Health Protection Awareness

The popular science books *Smog and Health Knowledge Q&A* and *Abnormal Weather and*

Environmental Pollution Events Cognition and Response were published as part of this project. The content was translated into various publicity materials including web pages, posters, and leaflets. Targeted health protection suggestions were promoted through display boards, websites, and news media. In a national survey, 430,000 parents received information about the prevention and control of childhood asthma. These efforts enhance the public's awareness of the health impact of air pollution and protective behaviours that can be adopted, thus playing an important role in reducing the health impact of air pollution.

NEXT RESEARCH DIRECTIONS

The atmosphere has a complex composition, and with the widespread application of new chemicals, people are exposed to an increasing number of novel air pollutants. Many studies have shown that health effects differ by air pollutant composition. It is still not clear how to accurately assess the health impact and health risk of single pollutants in mixed pollutant exposures. With the progress of science and the emergence of new air pollutants, future research should focus on several topics. First, health impact and mechanisms of action of new air pollutants and key components of particulate matter should be investigated to provide more evidence for causal health effects of air pollutants. Second, exposure characteristics and quantitative evaluation methods should be established for new air pollutants and air pollutant mixtures. This will provide accurate exposure data for the assessment of the health impact of pollutants. Third, a quantitative health risk assessment technology needs to be established to improve health protection intervention measures by assessing combined exposures of various air pollutants and the comprehensive influence of geographical, meteorological, population, and economic factors. Finally, the impact of continuous air quality improvement or deterioration on public health requires further investigation to support the establishment of a sustainable development path between economic development and ecological balance.

Conflicts of interest: No conflicts of interest.

Funding: The National Health and Family Planning Commission of the People's Republic of China (201402022). China National Key Technology R&D Program (2006BAI19B05), the National Natural Science Foundation of China (20977089, 81170255, 30570799, 81300013), Natural Science Foundation of Beijing Municipal (7164285).

doi: 10.46234/ccdcw2022.125

Corresponding author: Dongqun Xu, xudq@chinacdc.cn.

[1] China CDC Key Laboratory of Environment and Population Health, National Institute of Environmental Health, Chinese Center for Disease Control and Prevention, Beijing, China; [2] Academy of Military Medical Sciences, Academy of Military Sciences, Beijing, China; [3] Hubei Key Laboratory of Genetic Regulation and Integrative Biology, College of Life Sciences, Central China Normal University, Wuhan City, Hubei Province, China.

Submitted: February 14, 2022; Accepted: June 20, 2022

REFERENCES

1. Yang GH, Wang Y, Zeng YX, Gao GF, Liang XF, Zhou MG, et al. Rapid health transition in China, 1990-2010: findings from the global burden of disease study 2010. Lancet 2013;381(9882):1987 – 2015. http://dx.doi.org/10.1016/S0140-6736(13)61097-1.
2. Wang Q, Li LZ, Zhang YP, Cui Q, Fu YZ, Shi WY, et al. Research on the establishment and application of the environmental health indicator system of atmospheric pollution in China. Bull Environ Contam Toxicol 2021;106(1):225 – 34. http://dx.doi.org/10.1007/s00128-020-03084-5.
3. Deng T, Xie XM, Duan JF, Chen MQ. Exposure to diisononyl phthalate induced an increase in blood pressure through activation of the ACE/ AT1R axis and inhibition of NO production. Toxicol Lett 2019;309:42 – 50. http://dx.doi.org/10.1016/j.toxlet.2019.03.011.
4. Deng T, Xie XM, Duan JF, Chen MQ. Di-(2-ethylhexyl) phthalate induced an increase in blood pressure via activation of ACE and inhibition of the bradykinin-NO pathway. Environ Pollut 2019;247:927 – 34. http://dx.doi.org/10.1016/j.envpol.2019.01.099.
5. Xie XM, Deng T, Duan JF, Ding SM, Yuan JL, Chen MQ. Comparing the effects of diethylhexyl phthalate and dibutyl phthalate exposure on hypertension in mice. Ecotoxicol Environ Saf 2019;174:75 – 82. http://dx.doi.org/10.1016/j.ecoenv.2019.02.067.
6. Duan JF, Kang J, Qin W, Deng T, Liu H, Li BZ, et al. Exposure to formaldehyde and diisononyl phthalate exacerbate neuroinflammation through NF-κB activation in a mouse asthma model. Ecotoxicol Environ Saf 2018;163:356 – 64. http://dx.doi.org/10.1016/j.ecoenv.2018.07.089.
7. Zhu XM, Wang Q, Xing WW, Long MH, Fu WL, Xia WR, et al. $PM_{2.5}$ induces autophagy-mediated cell death via NOS2 signaling in human bronchial epithelium cells. Int J Biol Sci 2018;14(5):557 – 64. http://dx.doi.org/10.7150/ijbs.24546.
8. Xia WR, Fu WL, Wang Q, Zhu XM, Xing WW, Wang M, et al. Autophagy induced *FHL2* upregulation promotes IL-6 production by activating the NF-κB pathway in mouse aortic endothelial cells after exposure to $PM_{2.5}$. Int J Mol Sci 2017;18(7):1484. http://dx.doi.org/10.3390/ijms18071484.
9. Li N, Liu Z, Li YP, Li N, Chartier R, Mcwilliams A, et al. Estimation of $PM_{2.5}$ infiltration factors and personal exposure factors in two megacities, China. Build Environ 2019;149:297 – 304. http://dx.doi.org/10.1016/j.buildenv.2018.12.033.
10. Yang YB, Liu L, Xu CY, Li N, Liu Z, Wang Q, et al. Source apportionment and influencing factor analysis of residential indoor $PM_{2.5}$ in Beijing. Int J Environ Res Public Health 2018;15(4):686. http://dx.doi.org/10.3390/ijerph15040686.
11. Han JX, Chang JR, Liu JY, Meng CS, Xu DQ. First technical specifications for health risk assessment of ambient air pollution in China. China CDC Wkly 2021;3(33):706 – 9. http://dx.doi.org/10.46234/ccdcw2021.175.

Indexed by PubMed Central (PMC), Emerging Sources Citation Index (ESCI), Scopus, Chinese Scientific and Technical Papers and Citations, and Chinese Science Citation Database (CSCD)

The inauguration of *China CDC Weekly* is in part supported by Project for Enhancing International Impact of China STM Journals Category D (PIIJ2-D-04-(2018)) of China Association for Science and Technology (CAST).

CCDC weekly

Vol. 4 No. 26 Jul. 1, 2022

Responsible Authority
National Health Commission of the People's Republic of China

Sponsor
Chinese Center for Disease Control and Prevention

Editing and Publishing
China CDC Weekly Editorial Office
No.155 Changbai Road, Changping District, Beijing, China
Tel: 86-10-63150501, 63150701
Email: weekly@chinacdc.cn

CSSN
ISSN 2096-7071
CN 10-1629/R1